CHAPTER 3

DYNAMIC STABILITY OF BEAMS AND PLATES

3.1 GENERAL FORMULA TO PREDICT DYNAMIC STABILITY OF BEAMS SUBJECTED TO AXIAL PERIODIC LOADS

3.1.1 Introduction

The beam is one of the fundamental elements of an engineering structure. For example, the rockets and missiles with variable thrust time curve in the aerospace engineering and connecting rods, suspension systems in the mechanical/automobile engineering. Therefore, studying the dynamic stability behavior, of this simple structural component under time dependent axial loading would help in understanding and explaining the behavior of more complex, real structures. The periodicity of the loads are not distinctly seen for the dynamic stability of these structures, as an ideal case of the simple combination of the applied constant load and the periodic load. These ideal loads can be obtained by the Fourier or harmonic analysis of the thrust time curve using half range cosine series. Thus a time dependent thrust can be split into a constant load and a series of periodic loads with decreasing periods. The dynamic stability of the structural systems has to be analyzed at least for the combination of the constant part of the load and the periodic load with the highest period as this is the most critical periodic load for all practical purposes.

The energy methods provide accurate engineering solutions for the analysis of stability and vibration problems, for obtaining the critical load and the fundamental frequencies. This information is required to find the dynamic stability regions of structural members subjected to periodic loads, by the designers in the initial design phase. This method (energy method) is widely used where the displacement field of structural members is exact or approximate trigonometric or algebraic functions. It is necessary that the assumed functions chosen have to satisfy the geometric boundary conditions. In the present section, the regions of the dynamic stability behavior of the uniform, slender and isotropic beams subjected to periodic loads are studied with the classical boundary conditions.

In this section, the Euler – Bernoulli beam theory is used for the analysis, and an exhaustive study is carried out for the dynamic stability boundaries obtained for the simply supported (S-S), clamped-free (C-F), clamped-clamped (C-C) and clamped-simply supported (C-S) end conditions. In particular, one can obtain accurate solution even with single term trigonometric or a polynomial admissible function, which satisfy the geometric boundary conditions, with only one undetermined coefficient. In this section, to predict the dynamic stability behavior of uniform slender beams, subjected to the end axial periodic loads, with various boundary conditions, using the energy method. This simplifies

enormously the solution procedure for beams. This can be achieved from the energy method, which is successfully used in the FE Analysis [18]. Dynamic stability of beams is briefly discussed by Timoshenko and Gere [1]. Bolotin [17] discussed, in his classic work, the dynamic stability behavior of structural members including the beams using an analytical method. The first FE method to study the dynamic stability behavior of bars with various boundary conditions is due to Brown *et al.* [18]. In this study, the non-dimensional parameters chosen intuitively based on the similarity of the free vibration and buckling mode shapes.

The aim of the study in this section is to develop a formula to predict the dynamic stability behavior of beams where the mode shapes of the fundamental frequency and the buckling load are exact (same) or nearly the same, subjected to axial end periodic loads and is independent of the beam boundary conditions considered because of the specific proper non dimensional parameters derived using energy method. The advantage of using the present dynamic stability formula is that it is derived with mathematical rigor using the energy method, where as in the earlier study of Brown *et al.* [18] these non-dimensional parameters are chosen intuitively. This dynamic stability equation can be treated as a general dynamic stability formula valid for beams. The major contribution of the work in this section is to show the effectiveness of the formula to predict the dynamic stability behavior of beams, subjected to

axial periodic loads, is rigorously derived. If the requirement of the exactness of the mode shapes, but not the similarity as mentioned in Brown *et al.* [18], to obtain the dynamic stability curves is violated, one can obtain these dynamic stability curves with a small deviation and the error involved is directly dependent on the deviation of these mode shapes that can be assessed by calculating the corresponding L_2 norms.

3.1.2 Formulation

In this section the dynamic stability boundaries are derived for the uniform slender beam for the simply supported, clamped-free, clamped-clamped and clamped-simply supported boundary conditions using the energy method with assumed admissible function *'w'*.

For a uniform slender beam subjected to an end axial periodic loads as shown in Fig.3.1, the differential equation of equilibrium governing its dynamic stability by Bolotin [17], is

$$EI\frac{\partial^4 w}{\partial x^4} + P(t)\frac{\partial^2 w}{\partial x^2} + \overline{m}\frac{\partial^2 w}{\partial t^2} = 0 \qquad (3.1)$$

where E is Young's modulus, I is the area moment of inertia, L is the length of the beam and $\overline{m}$ is mass per unit length and $P(t)$ is the combination of constant and periodic loads.

In Eq. (3.1), $P(t)$ is defined as

$$P(t) = P_s + P_t \cos\theta t \qquad (3.2)$$

or

$$P(t) = \alpha P_{cr} + \beta P_{cr} \cos\theta t \tag{3.3}$$

where α and β are the dimensionless static load factor $(=\frac{P_s}{P_{cr}})$ and dimensionless dynamic load factor $(=\frac{P_t}{P_{cr}})$ respectively, P_s is the constant compressive load, P_t is the time dependent axial load, P_{cr} is the critical load, θ is the radian frequency associated with P_t and a relation exists between θ and ω, as $\frac{\theta}{2} = \omega$, at the onset of dynamic instability, ω is the natural frequency and t represents time.

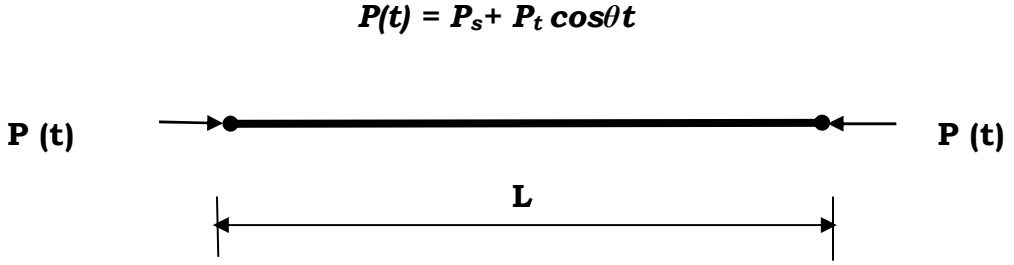

Fig.3.1 Uniform slender beam subjected to end concentrated axial Periodic load

Substituting Eq. (3.3) in Eq. (3.1), as

$$EI\frac{\partial^4 w}{\partial x^4} + (\alpha P_{cr} + \beta P_{cr}\cos\theta t)\frac{\partial^2 w}{\partial x^2} + \overline{m}\frac{\partial^2 w}{\partial t^2} = 0 \tag{3.4}$$

Assuming, a variable separable harmonic solution for w, as

$$w = f(x)\left[\bar{a}\sin\frac{\theta t}{2} + \bar{b}\cos\frac{\theta t}{2}\right] = w(x)w(t) \tag{3.5}$$

where $w(x)$ is the admissible function.

where $\bar{a}$ and $\bar{b}$ are constants and *f(x)* satisfy the boundary condition of the beam.

From the theory of linear equations with periodic coefficients [17, 18], the boundaries between the stable and unstable solutions are periodic solutions with periods T_t (time period) and $2T_t$. The regions of unstable solutions of the greatest practical importance are the ones bounded by the solutions with period $2T_t$.

Substituting Eq. (3.5) in Eq. (3.4), the principal regions of instability boundaries with a period of $2T_t$, using Bolotin [17] procedure will be

$$EI\frac{d^4 f(x)}{dx^4} + \left(P_s \pm \frac{P_t}{2}\right)\frac{d^2 f(x)}{dx^2} + \overline{m}\,\frac{\theta^2}{4} f(x) = 0 \qquad (3.6)$$

Equation (3.6) is the final differential equation governing the dynamic stability behavior of one dimensional structural element like beams. *f(x)* in Eq. (3.6) is a single term accurate admissible function.

The positive and negative signs associated with P_t give the two boundaries of the unstable regions in the dynamic stability phenomenon.

Equation (3.6) can also be obtained by using the variational formulation, the total potential energy functional Π is written as

$$\Pi = U - W - T \qquad (3.7)$$

or

$$\delta\Pi = \delta(U - W - T) = 0 \qquad (3.8)$$

where δ is the variational operator.

The expressions *U, W* and *T* in Eq. (3.7) are the strain energy, potential due to work and kinetic energy of the beam respectively, executing lateral harmonic vibrations, given by

$$U = \frac{EI}{2}\int_0^L \left(\frac{d^2w}{dx^2}\right)^2 dx \tag{3.9}$$

$$W = \frac{P(t)}{2}\int_0^L \left(\frac{dw}{dx}\right)^2 dx = \frac{1}{2}\left(\alpha \pm \frac{\beta}{2}\right) P_{cr}\int_0^L \left(\frac{dw}{dx}\right)^2 dx \tag{3.10}$$

and

$$T = \frac{1}{2}.\frac{\overline{m}\,\theta^2}{4}\int_0^L w^2 dx \tag{3.11}$$

where *w* is the admissible function.

Substituting, Eqs. (3.9) to (3.11) in Eq. (3.7), is written, as

$$\Pi = \frac{EI}{2}\int_0^L w^{"2} dx - \frac{P(t)}{2}\int_0^L w^{'2} dx - \frac{1}{2}\frac{\overline{m}\,\theta^2}{4}\int_0^L w^2 dx \tag{3.12}$$

In Eq. (3.12), prime and double prime denotes differentiation and double differentiation with respect to *x* (axial coordinate) respectively.

Taking the first variation of functional Π, and equating it to zero yields,

$$\delta\Pi = EI\int_0^L w^{"}\delta w^{"} dx - P(t)\int_0^L w^{'}\delta w^{'} dx - \overline{m}\,\frac{\theta^2}{4}\int_0^L w dw dx = 0 \tag{3.13}$$

In order to eliminate the variations $\delta w^{'}$ and $\delta w^{"}$ from Eq. (3.13), the first and second terms are integrated by parts [135, 136], after simplification, as

$$\delta\Pi = EI\left\{\left[w''\delta w'\right]_o^L - \left[w'''\delta w\right]_0^L\right\} + EI\int_0^L w''''\delta w dx - P(t)\left\{\left[w'\delta w\right]_0^L\right\} + P(t)\int_0^L w''\delta w dx - \overline{m}\,\omega^2\int_0^L w\,\delta w dx = 0 \tag{3.14}$$

Therefore, $\delta\Pi$ becomes

$$\delta\Pi = \int_0^L\left[EIw'''' + P(t)w'' - \overline{m}\frac{\theta^2}{4}w\right]\delta w dx - \left[EI\left\{\left[w'''\delta w\right]_0^L\right\} + P(t)\left\{\left[w'\delta w\right]_0^L\right\}\right] + EI\left[w''\delta w'\right]_o^L = 0 \tag{3.15}$$

Since the variation δw is arbitrary, the terms must vanish individually. Thus, the following equations are to be satisfied for the functional Π to attain an extremum value.

$$EIw'''' + P(t)w'' - \overline{m}\frac{\theta^2}{4}w = 0 \tag{3.16}$$

By substituting, $\frac{\theta^2}{4}w = -\frac{\partial^2 w}{\partial t^2}$ in the above equation, as

$$EI\frac{\partial^4 w}{\partial x^4} + P(t)\frac{\partial^2 w}{\partial x^2} + \overline{m}\frac{\partial^2 w}{\partial t^2} = 0 \tag{3.17}$$

The above equation is the same as that given in Eq. (3.6).

The dynamic stability equation for beams can be written in terms of energies, as

$$\Pi = \frac{EI}{2}\int_0^L\left(\frac{d^2w}{dx^2}\right)^2 dx - \frac{P(t)}{2}\int_0^L\left(\frac{dw}{dx}\right)^2 dx - \frac{\overline{m}}{2}\frac{\theta^2}{4}\int_0^L w^2 dx \tag{3.18}$$

The above equation is rewritten as

$$\Pi = \frac{EI}{2}\int_0^L\left(\frac{d^2w}{dx^2}\right)^2 dx - \left(P_s + P_t\cos\theta t\right)\frac{1}{2}\int_0^L\left(\frac{dw}{dx}\right)^2 dx - \frac{\overline{m}}{2}\frac{\theta^2}{4}\int_0^L w^2 dx \tag{3.19}$$

or

$$\Pi = \frac{EI}{2}\int_0^L \left(\frac{d^2w}{dx^2}\right)^2 dx - \left(\alpha \pm \frac{1}{2}\beta\right)\frac{P_{cr}}{2}\int_0^L \left(\frac{dw}{dx}\right)^2 dx - \frac{\overline{m}}{2}\frac{\theta^2}{4}\int_0^L w^2 dx \qquad (3.20)$$

If all the length quantities are non-dimensionalized with respect to the length of the beam, Eq. (3.20) rewritten, as

$$\Pi = \frac{EI}{2}\frac{1}{L}\int_0^1 \left(\frac{d^2\overline{w}}{d\overline{x}^2}\right)^2 d\overline{x} - \left(\alpha \pm \frac{1}{2}\beta\right)\frac{P_{cr}}{2}L\int_0^1 \left(\frac{d\overline{w}}{d\overline{x}}\right)^2 d\overline{x} - \frac{\overline{m}}{2}\frac{\theta^2}{4}L^3\int_0^1 \overline{w}^2 d\overline{x} \qquad (3.21)$$

where $\overline{w} = \frac{w}{L}$ and $\overline{x} = \frac{x}{L}$.

The lateral deflection in Eq. (3.5) is assumed for simply supported beam, using the single term standard exact trigonometric admissible function as

$$w = a\sin\frac{\pi x}{L} \qquad (3.22)$$

The lateral deflection w for the simply supported beam in the non-dimensional form as

$$\overline{w} = a\sin\pi\overline{x} \qquad (3.23)$$

where a is an undetermined coefficient.

Substituting, $\overline{w}$ in Eq. (3.21), and minimizing the total potential energy Π with respect to the undetermined coefficient a and equating it to zero, after simplification is written, as

$$\pi^4\frac{EI}{2}\frac{1}{L}\frac{1}{2}2a - \left(\alpha \pm \frac{\beta}{2}\right)\frac{\pi^2 P_{cr}}{2}L\frac{1}{2}2a - \frac{\overline{m}}{2}\frac{\theta^2}{4}L^3\frac{1}{2}2a = 0 \qquad (3.24)$$

Simplifying the above equation using Rayleigh's quotients, as

$$1-\left(\alpha \pm \frac{\beta}{2}\right)\lambda_b \frac{1}{RQ_1} - \frac{\theta^2}{4}\frac{\lambda_f}{\omega^2}\cdot\frac{1}{RQ_2} = 0 \tag{3.25}$$

where RQ_1 and RQ_2 are the Rayleigh's quotients and is given by

$$RQ_1 = \frac{\int_0^1 \left(\frac{d^2\bar{w}}{d\bar{x}^2}\right)^2 d\bar{x}}{\int_0^1 \left(\frac{d\bar{w}}{d\bar{x}}\right)^2 d\bar{x}} = \lambda_b \tag{3.26}$$

$$RQ_2 = \frac{\int_0^1 \left(\frac{d^2\bar{w}}{d\bar{x}^2}\right)^2 d\bar{x}}{\int_0^1 \bar{w}^2\, d\bar{x}} = \lambda_f \tag{3.27}$$

where λ_b and λ_f are the buckling load and frequency parameters respectively.

Substituting, Eqs. (3.26) and (3.27), in the Eq. (3.25) the equation governing the stability boundaries of the beams subjected to axial periodic loads at the ends is written as

$$1-\left(\alpha \pm \frac{\beta}{2}\right) - \frac{\theta^2}{4\omega^2} = 0 \tag{3.28}$$

Defining $\Omega = \frac{\theta}{\omega}$, Eq. (3.28) further simplified as

$$\frac{1}{4}\Omega^2 = (1-\alpha)\left(1 \pm \frac{\beta}{2(1-\alpha)}\right) = (1-\alpha)(1 \pm \mu) \tag{3.29}$$

where $\mu = \frac{\beta}{2(1-\alpha)}$

or

$$\Omega = 2\sqrt{(1-\alpha)(1\pm\mu)} \tag{3.30}$$

where Ω and μ are the nondimensional parameters used in Ref.[18] by intuition and are systematically obtained here.

Substituting, $\overline{w}$ for the clamped, cantilever and clamped-simply supported end conditions of the beam, as given in Table 3.1, in Eq.(3.21), and minimizing the total potential energy Π with respect to the undetermined coefficient a and equating it to zero, after simplification, is the same as the Eq.(3.30). In Eq. (3.30), the dynamic stability regions can be obtained for a given α, in terms of Ω and μ. These non-dimensional parameters (Ω and μ) are independent of the characteristic values of ω and P_{cr} of the beam considered and can be used as a general dynamic stability formula. However, to obtain the absolute values of the instability boundaries of a specific boundary condition of the beam, the corresponding values of ω and P_{cr} have to be used. The Eq. (3.30) is the solution for the dynamic stability regions of beam for any boundary condition. In this section, the formula is rigorously derived by energy method as the assumed admissible function w is used to obtain the fundamental frequency and critical load (for similar mode shapes).

3.1.2.2 Simply Supported Beam

The detailed procedure for the energy method is presented in this section for evaluating the fundamental frequency and buckling (critical) load parameters for a uniform beam subjected to axial periodic loads.

Equation (3.21), for the degenerate case of the buckling problem, becomes

$$\Pi = \frac{EI}{2}\frac{1}{L}\int_0^1 \left(\frac{d^2\overline{w}}{d\overline{x}^2}\right)^2 d\overline{x} - \frac{P_{cr}}{2}L\int_0^1 \left(\frac{d\overline{w}}{d\overline{x}}\right)^2 d\overline{x} \tag{3.31}$$

Substituting the expression $\overline{w}$ in Eq. (3.31), and minimizing the total potential energy Π with respect to the undetermined coefficient a and equating it to zero, after simplification, the buckling (critical) load parameter is obtained, as

$$\lambda_b = \frac{P_{cr}L^2}{EI} = \pi^2 \tag{3.32}$$

Equation (3.21) becomes for the vibration problem of the beam by neglecting the second term in Eq.(3.21), as

$$\Pi = \frac{EI}{2}\frac{1}{L}\int_0^1 \left(\frac{d^2\overline{w}}{d\overline{x}^2}\right)^2 d\overline{x} - \frac{\overline{m}}{2}\omega^2 L^3 \int_0^1 \overline{w}^2 d\overline{x} \tag{3.33}$$

Substituting the Eq. (3.23) in Eq. (3.33) and minimizing the total potential energy Π with respect to the undetermined coefficient a and equating it to zero, after simplification, the fundamental frequency parameter is obtained as,

$$\lambda_f = \frac{\overline{m}\,\omega^2 L^4}{EI} = \pi^4 \tag{3.34}$$

The similar procedure is followed to evaluate the buckling (critical) load parameters and fundamental frequency parameters for the clamped-clamped, clamped-free and clamped-simply supported end conditions of the beam. The buckling (critical) load and the fundamental frequency parameters for the above three end conditions are shown in Table 3.1.

3.1.3 Numerical Results and Discussion

The dynamic stability boundaries for a given beam is evaluated by using, Eq. (3.30), which are non dimensional, as

$$\Omega_1 = 2\sqrt{(1-\mu)(1-\alpha)} \tag{3.35}$$

and

$$\Omega_2 = 2\sqrt{(1+\mu)(1-\alpha)} \tag{3.36}$$

and between these values the beam is unstable. These stability regions are obtained by evaluating Ω_1 and Ω_2 for the values of μ varying from 0 to 0.5. These equations, Eq. (3.35) and Eq. (3.36) are independent of the beam boundary conditions. Thus, these equations give the general dynamic stability formula for beams. However, for a physical interpretation of the results obtained by Eq. (3.35) and Eq. (3.36), it is necessary to have the values of λ_b and λ_f for obtaining the principal instability regions. In this work, the buckling (critical) load parameter and the fundamental frequency parameter for beams are evaluated by using the standard single term admissible trigonometric functions '*w*',

simplified for one dimensional problem are given in Table 3.1, for various boundary conditions.

The data available on the mode shapes can be used to find out whether the mode shapes vary very little by physical observation of the same. If mathematical rigor is required, this difference can be found by comparing the L_2 Norm [79] of the respective mode shapes, thereby removing the subjective ness of deciding the difference by physical observation. The commonly used trigonometric functions in the analytical studies for the simply supported, clamped, cantilever and clamped-simply supported beams are given in Table 3.1. Table 3.2 presents the values of L_2 norm obtained from the FE and analytical assumed mode shapes for classical boundary conditions of the beam. The percentage of error in the use of assumed mode shapes with reference to the FE solution for these boundary configurations is discussed using the L_2 norm in Table 3.3. The percentage error in the L_2 norm, given in Table 3.3 clearly indicates that the assumed analytical mode shapes for simply supported beam is exact with reference to the buckling and vibration problems, where as the other functions for the clamped and clamped-free beams are exact for the buckling mode only and a small percentage of error exists in vibration mode shapes. In case of the clamped-simply supported boundary condition, a small percentage of error exists with reference to the buckling and vibration mode shapes.

A single term admissible function chosen for the evaluation of the critical load and fundamental frequency, the intuitive condition used in Brown *et al.* [18] is satisfied exactly in the present energy method. Table 3.4 gives the dynamic stability boundaries Ω_1 and Ω_2 of beams, for any boundary condition for the value of μ varying from 0 to 0.5 and for the values of α = 0.0, 0.5 and 0.8. It is seen from the Table 3.4 that the digitized values from the graphical representation of Brown *et al.* [18] are in good agreement compared to the results obtained in the present work. Table 3.5 shows the percentage of error between the results obtained from the present formula and those given in Brown *et al.* [18], using FE method, has a maximum error margin of around 2.8%. Figure 3.7 shows the general dynamic stability curves for the given beam using present formula.

3.2 DYNAMIC STABILITY OF BEAMS ON ONE PARAMETER (WINKLER MODEL) ELASTIC FOUNDATION

With the knowledge gained from the previous section 3.1, the dynamic stability behavior of simply supported beam resting on an elastic foundation is investigated in this section. To decrease the regions of dynamic instability of beams, it is necessary to investigate the effect of the elastic foundation on the regions of dynamic stability, an aspect to be considered in the initial phase of design. The energy method, provide a convenient means to evaluate the buckling load and fundamental frequency parameters and the accuracy of the solution, depends on the chosen admissible function for the lateral deflection. Assumed single term trigonometric admissible functions are to satisfy the boundary conditions involved in the problem. Beams on elastic foundation are commonly used in many fields of engineering. The motivation of the present section is to develop a simple and accurate formula, for the dynamic stability regions of simply supported beam resting on the elastic foundation, subjected to end axial periodic loads. Brown *et al.* [18], studied the dynamic stability of slender bars, subjected to pulsating concentrated periodic axial load, using FE method. The dynamic stability of beams resting on an elastic foundation is investigated by Abbas & Thomas [28], the effect of the elastic foundation on the boundaries of dynamic stability reported in their study. It is also reported that as the foundation parameter increases, the width of the regions of dynamic stability decreases and the regions of dynamic

stability shifts away from the vertical axis. Hence, the beam is less sensitive to period loads. Brown *et al.* [18], are shown in their study that the mode shapes of the buckling of uniform bars resting on elastic foundation depends on the value of foundation stiffness parameter. There exists a transition foundation stiffness value, beyond this transition foundation stiffness value, the mode shape for the buckling changes. In the case of simply supported beam, the buckling and the vibration modes are same (one–half sine wave) when the foundation parameter is below the first transition foundation parameter. These mode shapes will differ when the foundation parameter above the first transition value (two – half sine waves for buckling and one half–sine wave for the free vibration problems). Timoshenko and Gere [1] found that for simply supported beam, the value of the first transition foundation parameter is 4. Further, it is shown that the transmission foundation parameter does not exist for the vibration mode shapes of beams resting on an elastic foundation [35].

In spite of many studies on the dynamic stability behavior of beams resting on an elastic foundation subjected to end axial periodic load problems. In this section the effect of elastic foundation on the dynamic stability boundaries for the simply supported beam, resting on an elastic foundation, subjected to end axial periodic loads are studied. The effect on the dynamic stability regions, when changing the mode

shapes for stability and vibration with increasing the value of foundation parameter is studied in this section. Euler –Bernoulli beam theory used for the analysis in the present study.

3.2.1 Formulation

In this section the dynamic stability behavior of simply supported beam resting on an elastic foundation, a formula is derived using energy method. For a uniform beam resting on an elastic foundation, subjected to concentrated end axial periodic loads P(t), as shown in Fig. 3.2, the total potential energy Π is given by

$$\Pi = U + U_F - T - W \tag{3.37}$$

where U, U_F, W and T are the strain energy, energy stored in the foundation, potential due to work and kinetic energy respectively.

$$U_F = \frac{k}{2}\int_0^L w^2 dx \tag{3.38}$$

where k is the elastic foundation stiffness.

Substituting, energies and potential due to work in Eq. (3.37), the total potential energy for the dynamic stability problem of the beam resting on an elastic foundation, is

$$\Pi = \frac{EI}{2}\int_0^L w''^2 dx + \frac{k}{2}\int_0^L w^2 dx - \frac{P(t)}{2}\int_0^L w'^2 dx - \frac{1}{2}\frac{\overline{m}\theta^2}{4}\int_0^L w^2 dx \tag{3.39}$$

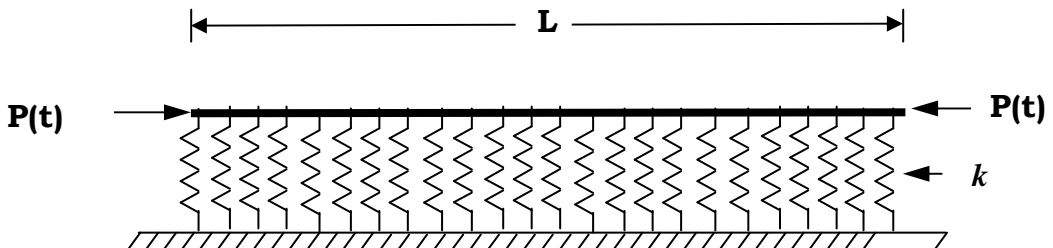

Fig.3.2 Uniform simply supported beam on elastic foundation subjected to axial concentrated periodic loads.

Substituting *P (t)* value from Eq.(3.2), in Eq. (3.39), becomes

$$\Pi = \frac{EI}{2}\int_0^L w''^2 dx + \frac{k}{2}\int_0^L w^2 dx - \left(\alpha \pm \frac{\beta}{2}\right)\frac{P_{cr}}{2}\int_0^L w'^2 dx - \frac{1}{2}\frac{\overline{m}\,\theta^2}{4}\int_0^L w^2 dx \qquad (3.40)$$

For the buckling problems of the beams on the uniform elastic foundation the Eq. (3.40) becomes in the non dimensional form is

$$\Pi = \frac{EI}{2L}\int_0^1 \overline{w}''^2 d\bar{x} + \frac{kL^3}{2}\int_0^1 \overline{w}^2 d\bar{x} - \frac{P(t)\,L}{2}\int_0^1 \overline{w}'^2 d\bar{x} \qquad (3.41)$$

The lateral deflection for the simply supported beam in the non-dimensional form as given in the Eq. (3.23) is written in terms of mode number, as

$$\overline{w} = a\sin m\pi\bar{x}$$

Substituting $\overline{w}$ in Eq. (3.41) and minimizing the total potential energy Π with respect to the undetermined coefficient *a* and equating it to zero, after simplification, the critical load P_{cr} is obtained as

$$P_{cr} = \frac{EI}{L^2}\pi^2\left(m^2 + \frac{\gamma}{m^2}\right) \qquad (3.42)$$

The buckling (critical) load parameter is

$$\lambda_b = \frac{P_{cr} L^2}{EI} = \pi^2 \left(m^2 + \frac{\gamma}{m^2} \right) \tag{3.43}$$

where γ is the elastic foundation parameter ($= \frac{kL^4}{\pi^4 EI}$).

The total potential energy Π in the case of the vibration problem of uniform beam resting on an elastic foundation, the Eq.(3.40) becomes in the non-dimensional form, as

$$\Pi = \frac{EI}{2L} \int_0^1 \overline{w}''^2 d\overline{x} + \frac{kL^3}{2} \int_0^1 \overline{w}^2 d\overline{x} - \frac{\overline{m}\,\omega^2}{2} L^3 \int_0^1 \overline{w}^2 d\overline{x} \tag{3.44}$$

The same procedure is adopted for the vibration problem on the uniform elastic foundation and minimizing the total potential energy Π with respect to the undetermined coefficient *a* and equating it to zero, after simplification, the frequency parameter is obtained as

$$\lambda_f = \frac{\overline{m}\,\omega^2 L^4}{EI} = \pi^4 \left(m^2 + \frac{\gamma}{m^2} \right) \tag{3.45}$$

Substituting Eq. (3.22) in Eq. (3.40) and minimizing the total potential energy Π with respect to the undetermined coefficient *a* and equating it to zero, by substituting the values, $P_{cr} = \frac{\pi^2 EI}{L^2}$ and $\overline{m} = \frac{\pi^4 EI}{\omega^2 L^4}$ without considering the foundation for critical load and frequency for the first mode, after simplification, the dynamic stability equation, as

$$1 + \gamma - \left(\alpha \pm \frac{\beta}{2} \right) - \frac{\theta^2}{4\omega^2} = 0 \tag{3.46}$$

The Eq.(3.46) is called the dynamic stability formula for the simply supported beam resting on an elastic foundation.

The Eq. (3.46) simplified as

$$\Omega = 2\sqrt{(1-\alpha)(1\pm\mu)+\gamma} \tag{3.47}$$

From Eq. (3.47) the dynamic stability regions can be evaluated for a given α and γ, in terms of Ω and μ.

3.2.1.1 Evaluation of Transition Foundation

The transition value of the foundation parameter γ_{Ti} (i varies from 1, 2, 3,..), and corresponding to the buckling mode number (m_b), where the buckling load parameter λ_b changes from mode m_b to mode $(m+1)_b$. The transition value γ_{Ti} is evaluated from the equation, given by Timoshenko and Gere [1], using the condition that the buckling load parameters are the same for two consecutive modes of buckling m_b and $(m+1)_b$, as

$$\lambda_{bm} = \lambda_{b(m+1)} \tag{3.48}$$

The value of the γ_{Ti} are

$$\gamma_{Ti} = m_b^{\,2}(m+1)_b^{\,2} \quad , \quad (i,\ m_b = 1, 2, 3, 4\ldots) \tag{3.49}$$

The values of γ_{Ti} for the buckling problem are 4, 36, 144 …….. for (i =1, 2, 3…….).

Substituting, Eq. (3.23) in Eq. (3.41) and minimizing the total potential energy Π with respect to the undetermined coefficient a and equating it to zero, the critical load P_{cr} (for two half sine waves of the stability) becomes

$$P_{cr} = 4\frac{\pi^2 EI}{L^2}\left[1+\frac{\gamma}{16}\right] \tag{3.50}$$

and the buckling load parameter, as

$$\lambda_b = \frac{P_{cr}L^2}{EI} = \pi^2\left(4+\frac{\gamma}{4}\right) \tag{3.51}$$

Similarly, substituting Eq.(3.22) in Eq.(3.40) for the simply supported beam and minimizing the total potential energy Π with respect to the undetermined coefficient *a* and equating it to zero, after simplification, the dynamic stability equation for mode shapes (two-half sine waves for the stability and one-half sine wave for vibration) is obtained, as

$$1-\frac{\left(\alpha\pm\frac{\beta}{2}\right)P_{cr}.4\frac{\pi^2}{L^2}}{\frac{\pi^4 EI}{L^4}\left[16+\frac{kL^4}{\pi^4 EI}\right]}-\frac{\frac{\overline{m}\,\theta^2}{4}}{\frac{\pi^4 EI}{L^4}\left[1+\frac{kL^4}{\pi^4 EI}\right]}=0 \tag{3.52}$$

Substituting, $P_{cr}=\frac{4\pi^2 EI}{L^2}$ and $\overline{m}=\frac{\pi^4 EI}{\omega^2 L^4}$ in Eq.(3.52) for two-half sine waves for the stability and one-half sine wave for vibration without consideration of the foundation for critical load and frequency, after simplification the dynamic stability equation for mode shapes (two-half sine waves for stability and one-half sine wave for vibration) is obtained, as

$$1-\left(\alpha\pm\frac{\beta}{2}\right)\left(\frac{1}{1+\frac{\gamma}{16}}\right)-\frac{\theta^2}{4\omega^2(1+\gamma)}=0 \tag{3.53}$$

The Eq.(3.53) simplified as

$$\Omega = \frac{\theta}{\omega} = 2\sqrt{\left[(1-\alpha)(1\pm\mu)+\frac{\gamma}{16}\right]\left[\frac{(1+\gamma)}{(1+(\gamma/16))}\right]} \tag{3.54}$$

From Eq. (3.54), the dynamic stability regions can be obtained for (two half sine waves for stability and one half sine wave for vibration) for a given α and γ for the foundation parameter greater than the first transition (γ_{T1} = 4) in terms of Ω and μ.

Substituting, Eq. (3.22) in Eq. (3.40) and minimizing the total potential energy Π with respect to the undetermined coefficient *a* and equating it to zero, with consideration of foundation for the critical load, without consideration of the foundation for frequency for one-half sine wave for both stability and vibration, after simplification, as

$$\Omega = \frac{\theta}{\omega} = 2\sqrt{(1-\alpha)(1\pm\mu)(1+\gamma)} \tag{3.55}$$

Substituting, Eq. (3.22) in Eq. (3.40) and minimizing the total potential energy Π with respect to the undetermined coefficient *a* and equating it to zero, the value of critical load with consideration of foundation for two-half sine waves and frequency without consideration of foundation for one-half sine wave, after simplification, obtained as

$$\Omega = \frac{\theta}{\omega} = 2\sqrt{(1-\alpha)(1\pm\mu)(1+\gamma)} \tag{3.56}$$

Substituting, Eq.(3.22) in Eq.(3.40) for the simply supported beam and minimizing the total potential energy Π with respect to the undetermined coefficient *a* and equating it to zero, the values of critical

load and frequency for one-half sine wave for both stability and vibration, and two-half sine waves for both stability and vibration, with consideration of the foundation, after simplification, obtained as

$$\Omega = \frac{\theta}{\omega} = 2\sqrt{(1-\alpha)(1\pm\mu)} \tag{3.57}$$

3.2.2 Numerical Results and Discussion

The formula developed in this section to investigate the dynamic stability boundaries of simply supported beam resting on an elastic foundation and in the non dimensional form the characteristic values of the beam such as the fundamental frequency and the buckling load parameters do not appear explicitly. However, these characteristic values appear implicitly in the definition of the non dimensional parameters μ and Ω.

Table 3.6 gives the values of the stability boundaries Ω_1 and Ω_2 between which it is dynamically unstable with varying μ, with the mode shape of one half sine wave for both the stability and vibration problems for $\gamma = 1$. Table 3.7 gives the values of stability boundaries Ω_1 and Ω_2 with varying β instead of μ proposed here, with the mode shape of one half sine wave for both the stability and vibration problems for $\gamma = 2$. The dynamic stability results of Abbas and Thomas [28], for a slender beam resting on an elastic foundation are also included in this Table. Since the non dimensional parameter given in Abbas and Thomas [28] is β instead

of μ proposed here, and is difficult to convert β to μ due to lack of sufficient information, the values of μ converted to β for the results presented in Table 3.7. Table 3.8 shows the comparative results with Abbas and Thomas [28]. One can see the good agreement between the results obtained from the present formula and those given in [28] obtained using the finite element method for α = 0.5, with a maximum error of around 2%. Table 3.9 give the values of the stability boundaries Ω_1 and Ω_2 between which it is dynamically unstable for varying μ, for the mode shape of one half sine wave for both the stability and vibration problems for γ = 3. Figures 3.8 to 3.10 shows the instability boundaries Ω_1 and Ω_2 given in Tables 3.6, 3.7 and 3.9 respectively, considering the reference buckling load and frequency parameters, are without consideration of the elastic foundation, for the values of α = 0.0, 0.5 and 0.8. It is observed that with the increasing elastic foundation parameter, the dynamic stability regions shifts away from the vertical axis and decreases the regions of dynamic instability.

Table 3.10 gives values of the stability boundaries Ω_1 and Ω_2 for two half sine waves for the stability problem and one half sine wave for the vibration problem above the first transition foundation parameter (γ>4) for γ = 4.5, obtained from Eq.(3.54) with reference buckling (critical) load and frequency parameters obtained without consideration of the elastic foundation. Figure 3.11 shows the instability boundaries of the

beam for the values given in Table 3.10. Table 3.11 gives the dynamic stability boundaries Ω_1 and Ω_2, obtained from Eq. (3.55) below the first transition value $\gamma = 2$, for one half sine wave for the stability problem with consideration of the elastic foundation for the reference critical load and for the vibration problem without consideration of the elastic foundation for the reference frequency and the dynamic stability results presented in the digital form in the Table 3.11 are also given in analogue form in Fig.3.12.

Table 3.12 gives the values of the stability boundaries Ω_1 and Ω_2 for two half sine waves for stability and one half sine wave for the vibration, reference buckling load parameter with consideration of elastic foundation (γ=4.5) and reference frequency parameter without consideration of the elastic foundation above the first transition value are obtained from Eq. (3.56) and the instability boundaries in the analogue form are shown in Fig. 3.13.

The dynamic stability boundaries for the value of the foundation parameter below the first transition value ($\gamma < 4$) with one half sine wave and above the first transition value ($\gamma > 4$) with two half sine waves for both the stability and vibration problems, obtained from Eq. (3.57), are presented with reference buckling (critical) load and frequency parameters considering the elastic foundation. Eq. (3. 57) derived here is

the same as that given in Eq. (3.30) in the section 3.1. It can be seen from the present results that are converted to the non dimensional form used in Abbas and Thomas [28] that the dynamic stability curves obtained by the others and the general dynamic stability curves presented in the present work give the same trend, thus showing the advantage of the non dimensional parameters used in this study and are shown in Fig.3.7.

3.3 DYNAMIC STABILITY OF BEAMS ON TWO PARAMETER (PASTERNAK MODEL) ELASTIC FOUNDATION

With the knowledge gained from the previous sections 3.1 and 3.2, the dynamic stability of simply supported beam resting on Pasternak foundation considering the effect of first transition foundation parameter is presented in this section. The study of the dynamic instability boundaries of Euler-Bernoulli beam resting on the two parameter elastic foundations subjected to an end concentrated axial periodic loads is an important input for structural design engineers, which is used in many fields of engineering. One parameter Winkler model of the elastic foundation is widely used, because of simplicity. The Winkler foundation, consists of an infinitely large number of closely spaced elastic springs and neglects the interaction between the adjacent elastic springs and hence it cannot represent the true characteristics of many practical foundations, to overcome this, two parameter elastic foundation are used. The earlier researchers, Filonenko-Borodich [59], Pasternak [60] and Kerr[61] assumed that the formulation represented by the two parameter elastic foundation are present to get a realistic insight about the response of the actual behavior of the structural members on two parameter elastic foundation. A brief review of the various types of two parameter foundations is given by Zhaohua and Cook [62] that can be used for a quick reference to the two parameter elastic foundations. But, out of all, the two parameter elastic foundations described in their study,

the Pasternak foundation is used for its analytical simplicity. In this section, the dynamic stability behavior of simply supported uniform, isotropic and homogeneous beam is considered. The simply supported beam is chosen because of the availability of the single term exact trigonometric admissible function that can be used to obtain the exact dynamic stability solution by employing the energy method for prediction of the dynamic stability behavior, because of the interferences drawn, they are accurate.

In general, the two parameter foundation for one dimensional problem like beams are mathematically represented by

$$p(x) = k_1 w(x) - k_2 \frac{d^2 w(x)}{dx^2} \tag{3.58}$$

where *p(x)* is the pressure exerted by using the elastic foundation on the beam for a lateral deflection w, x is the axial coordinate, k_1 is the first foundation stiffness (or Winkler stiffness) and k_2 is the second foundation stiffness with different physical interpretation associated with respect to the second foundation parameter of the two parameter foundations discussed in Zhaohua and Cook [62]. For the Pasternak foundation, k_2 is the shear layer stiffness which represents the foundation model. The buckling and the vibration analysis of the beams on the Pasternak foundation are studied in the work of Rao and Raju [68].

Another important phenomenon in the buckling problem of the beams is the change of mode shapes of buckling at discrete value of the first foundation parameter of the Pasternak foundation. This phenomenon for the Winkler foundation is discussed by Timoshenko and Gere [1]. It is found that for a simply supported beam the value of this first transition foundation parameter in case of the Pasternak foundation, for the buckling problem, is dependent on the first foundation parameter only [1]. Further, it is also shown that such a transition foundation parameter does not exist for the mode shape change in the vibration problems of beams on the Pasternak foundation by Rao [65]. As it is mentioned earlier that the emphasis, in the present study is on the simply supported beams only and for other boundary conditions, analytical expressions for the transition foundation parameters cannot be easily evaluated as the transition phenomenon is complex [52].

The effect of the transition buckling mode shapes on the dynamic stability regions of the simply supported beam is clearly brought out in this study. The use of different reference values for evaluating the buckling (critical) load and the frequency parameters on the dynamic instability regions is discussed in this work. Finally, the existence of an elegant general dynamic instability formula is established for the simply

supported beams on the Pasternak foundation with particular emphasis on the effect of the first transition foundation parameter.

3.3.1 Dynamic Stability Equation

In this section, the dynamic stability of simply supported beam resting on a two parameter elastic foundation formula is derived using the energy method with assumed single term accurate admissible function *'w'*. The structural member, used in this section is a simply supported beam on the Pasternak foundation subjected to the end axial periodic loads, as shown in Fig.3.3

The instability regions can be obtained, neglecting damping, following the classical work of Bolotin [17], as

$$[K]\{\delta\}-\left[P_s \pm \frac{P_t}{2}\right][G]\{\delta\}-\frac{\theta^2}{4}[M]\{\delta\}=0 \tag{3.59}$$

where [K], [G] and [M] are the system stiffness matrix, system geometric stiffness matrix and system mass matrix respectively and {δ} is the eigenvector.

Post multiplying Eq. (3.59) by $\frac{1}{2}\{\delta\}^T$, we get

$$\frac{1}{2}\{\delta\}^T[K]\{\delta\}-\frac{1}{2}\left[P_s \pm \frac{P_t}{2}\right]\{\delta\}^T[G]\{\delta\}-\frac{1}{2}\frac{\theta^2}{4}\{\delta\}^T[M]\{\delta\}=0 \tag{3.60}$$

Equation (3.60) represents the energy equation corresponding to Eq. (3.59), and is written as

$$\Pi = U_P - W - T \tag{3.61}$$

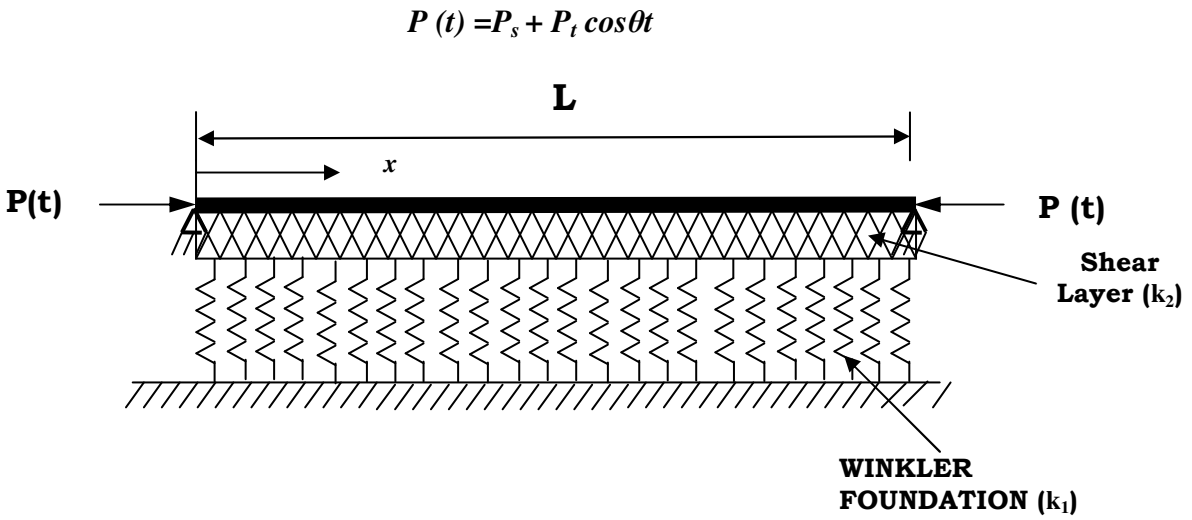

Fig. 3.3 Uniform simply supported beam on Pasternak Foundation subjected to axial Periodic loads.

where U_P is combined strain energy U and the energy U_{PF} stored in the Pasternak foundation, W is the potential due to work and T is the kinetic energy.

$$U_P = U + U_{PF} \tag{3.62}$$

The energy stored in the Pasternak foundation is written as

$$U_{PF} = \frac{k_1}{2}\int_0^L w^2 dx + \frac{k_2}{2}\int_0^L w'^2 dx \tag{3.63}$$

where k_1 and k_2 are the Winkler foundation stiffness and shear layer foundation stiffness.

Substituting, the energies and potential due to work in Eq.(3.61), the following equation is obtained as

$$\Pi = \frac{EI}{2}\int_0^L w''^2 dx + \frac{k_1}{2}\int_0^L w^2 dx + \frac{k_2}{2}\int_0^L w'^2 dx - \frac{1}{2}\left(P_s \pm \frac{P_t}{2}\right)\int_0^L w'^2 dx - \frac{1}{2}\frac{\overline{m}\theta^2}{4}\int_0^L w^2 dx \tag{3.64}$$

Non-dimensionalizing the Eq. (3.64), all the length quantities with respect to the length of the beam *L*, we get

$$\Pi = \frac{1}{2}\int_0^1 \overline{w}''^2 d\overline{x} + \frac{k_1 L^4}{EI}\frac{1}{2}\int_0^1 \overline{w}^2 d\overline{x} + \frac{k_2 L^2}{EI}\frac{1}{2}\int_0^1 \overline{w}'^2 d\overline{x} - \frac{1}{2}\left(P_s \pm \frac{P_t}{2}\right)\frac{L^2}{EI}\int_0^1 \overline{w}'^2 d\overline{x} - \frac{1}{2}\frac{\overline{m}\theta^2 L^4}{4EI}\int_0^1 \overline{w}^2 d\overline{x} \tag{3.65}$$

where $\overline{w} = w/L$ and $\overline{x} = x/L$

Equation (3.65) is the general dynamic stability equation that can be solved by proper non-dimensionalization of the loads P_s, P_t and the applied radian frequency θ with the corresponding reference values P_{cr} and ω, where these values are the critical (buckling) load and radian frequency of the beam, chosen with or without considering the effect of Pasternak foundation. These reference values play an important role in interpreting the dynamic instability regions, and is shown later that a particular set of the reference values give the elegant general dynamic instability regions that are invariant with the other non-dimensionalized parameters of the dynamic stability problem.

3.3.1.1 Evaluation of buckling (critical) load and frequency parameters

Equation (3.65) is the basic dynamic stability equation from which the matrix equation for the free vibration and the buckling problems can be deduced as the special cases, by neglecting the kinetic energy term

(*T)*, for the degenerate case of the buckling problem, the beam resting on Pasternak foundation, the Eq.(3.65), becomes

$$\Pi = \int_0^1 \overline{w}''^2 d\bar{x} + \frac{k_1 L^4}{EI}\int_0^1 \overline{w}^2 d\bar{x} + \frac{k_2 L^2}{EI}\int_0^1 \overline{w}'^2 d\bar{x} - \frac{P_{cr} L^2}{EI}\int_0^1 \overline{w}'^2 d\bar{x} \qquad (3.66)$$

and

For the degenerate case of the free vibration problem, the beam resting on Pasternak foundation, the Eq.(3.65), becomes

$$\Pi = \int_0^1 \overline{w}''^2 d\bar{x} + \frac{k_1 L^4}{EI}\int_0^1 \overline{w}^2 d\bar{x} + \frac{k_2 L^2}{EI}\int_0^1 \overline{w}'^2 d\bar{x} - \frac{\overline{m}\,\omega^2 L^4}{EI}\int_0^1 \overline{w}^2 d\bar{x} \qquad (3.67)$$

The solutions of Eqs. (3.66) and (3.67) gives the Euler buckling load and the frequency parameters including the effect of the Pasternak foundation.

Using the single term standard exact trigonometric admissible function for the lateral deflection *w* for the simply supported beam, in the non-dimensional form as given in Eq. (3.23) is written in terms of mode number, as

$$\overline{w} = a \sin m\pi\bar{x}$$

Substituting, the expression $\overline{w}$ in Eq. (3.66) and Eq. (3.67), and minimizing the total potential energy Π with respect to the undetermined coefficient *a* and equating it to zero, after simplification, the buckling load and the frequency parameters are obtained in terms of the mode number m_b and m_f, denoted by m_b for the buckling and m_f for the free vibration problem respectively, as

$$\lambda_b = \frac{P_{cr}L^2}{EI} = \pi^2(m_b{}^2 + \frac{\gamma_{F_1}}{m_b{}^2} + \gamma_{F_2}) \tag{3.68}$$

and

$$\lambda_f = \frac{\overline{m}\,\omega^2 L^4}{EI} = \pi^4(m_f{}^4 + \gamma_{F_1} + m_f{}^2\gamma_{F_2}) \tag{3.69}$$

where the first and second foundation parameters are $\gamma_{F_1} = \frac{k_1 L^4}{\pi^4 EI}$ and $\gamma_{F_2} = \frac{k_2 L^2}{\pi^2 EI}$ respectively, λ_b is the buckling load parameter (= $\frac{P_{cr}L^2}{EI}$)and λ_f is the natural frequency parameter (= $\frac{\overline{m}\,\omega^2 L^4}{EI}$).

3.3.1.2 Transition values of the foundation parameter

The transition value of the foundation parameter $\gamma_{T\,i}$ (*i* varies from 1, 2, 3,...., and corresponding to the buckling mode number m_b), where the buckling load parameter λ_b changes from mode m_b to mode $(m+1)_b$. The transition value $\gamma_{T\,i}$ is evaluated from Eq. (3.68), using the condition that the buckling load parameters are the same for two consecutive modes of the buckling m_b and $(m+1)_b$, as given in the Eq.(3.48)

The value of γ_{Ti} are

$$\gamma_{Ti} = m_b{}^2(m+1)_b{}^2 \quad , \qquad (\text{i, } m_b = 1,\ 2,\ 3,\ 4\ldots) \tag{3.70}$$

Two significant observations from the evaluation of γ_{Ti} are

a) the contribution for γ_{Ti} for the buckling problem, is from the first foundation parameter γ_{F_1} only without any contribution of γ_{F_2} and

b) A similar equation as Eq. (3.70) for the phenomenon of transition does not exist for the free vibration problem, where the mode shapes change.

The values of γ_{Ti} for the buckling problem are 4, 36, 144 …….. for (i =1, 2, 3…….). In the present study the effect of the first transition foundation parameter γ_{T1} = 4 and its effect on the dynamic stability regions of the simply supported beam is investigated in detail.

3.3.1.3. Variation of λ_b and λ_f for different values of m_b and m_f.

Equations (3.68) and (3.69), give the expressions for λ_b and λ_f for different values of m_b, m_f, γ_{F_1} and γ_{F_2}. Depending on these values of γ_{F_1}, γ_{F_2}, m_b and m_f, the expressions for λ_b and λ_f are evaluated concisely and presented here:

a) For $\gamma_{F_1} < \gamma_{T1}$ ($m_b = m_f = 1$)

The expressions for λ_b and λ_f are

$$\lambda_b = \frac{P_{cr} L^2}{EI} = \pi^2 \left[1 + \gamma_{F_1} + \gamma_{F_2}\right] \tag{3.71}$$

and

$$\lambda_f = \frac{\overline{m}\,\omega^2 L^4}{EI} = \pi^4 (1 + \gamma_{F_1} + \gamma_{F_2}) \tag{3.72}$$

b) $\gamma_{F_1} > \gamma_{T1}$ and $\gamma_{F_1} < \gamma_{T2}$ (m_b =2, m_f =1)

These expressions are

$$\lambda_b = \frac{P_{cr}L^2}{EI} = \pi^2\left[4 + \frac{\gamma_{F_1}}{4} + \gamma_{F_2}\right] \tag{3.73}$$

and

$$\lambda_f = \frac{\overline{m}\,\omega^2 L^4}{EI} = \pi^4(1 + \gamma_{F_1} + \gamma_{F_2}) \tag{3.74}$$

c) $\gamma_{F_1} > \gamma_{T1}$ and $\gamma_{F_1} < \gamma_{T2}$ (m_b = 2, m_f = 2)

The expressions for λ_b and λ_f are

$$\lambda_b = \frac{P_{cr}L^2}{EI} = \pi^2\left[4 + \frac{\gamma_{F_1}}{4} + \gamma_{F_2}\right] \tag{3.75}$$

and

$$\lambda_f = \frac{\overline{m}\,\omega^2 L^4}{EI} = \pi^4(16 + \gamma_{F_1} + 4\gamma_{F_2}) \tag{3.76}$$

Though the expressions for λ_b and λ_f for the three cases considered here are given for the sake of completeness, for any combination of m_b, m_f, γ_{F_1} and γ_{F_2} the buckling and frequency parameters can be straight away obtained for any given value of these four parameters, taking care of the transition value of the foundation parameter for γ_{F_1}.

3.3.2 Concise Form of Dynamic Stability Formulas

The dynamic stability formulas can be concisely written, by using the reference values of P_{cr} and ω obtained for different values of γ_{F_1} and γ_{F_2}

with the consideration of the proper values of m_b and m_f. The concise formulas for predicting the dynamic instability regions of the simply supported beam on the Pasternak foundation are:

a) Substituting Eq. (3.23) in Eq. (3.65), and minimizing the total potential energy Π with respect to the undetermined coefficient a and equating it to zero, using the first mode of buckling and free vibration (m_b = m_f =1) as the reference values, where $P_{cr} = \frac{\pi^2 EI}{L^2}$ and $\overline{m} = \frac{\pi^4 EI}{\omega^2 L^4}$ obtained without considering the effect of Pasternak foundation, after simplification, the following dynamic stability formula is obtained as

$$1 + \gamma_{F_1} + \gamma_{F_2} - \left(\alpha \pm \frac{\beta}{2} \right) - \frac{\theta^2}{4\omega^2} = 0 \tag{3.77}$$

where $\alpha = \frac{P_s}{P_{cr}}$, $\beta = \frac{P_t}{P_{cr}}$, $\gamma_{F_1} = \frac{k_1 L^4}{\pi^4 EI}$ and $\gamma_{F_2} = \frac{k_2 L^2}{\pi^2 EI}$

or

$$\Omega = \frac{\theta}{\omega} = 2\sqrt{(1-\alpha)(1 \pm \mu) + \gamma_{F_1} + \gamma_{F_2}} \tag{3.78}$$

b) Substituting Eqs. (3.23) in Eq. (3.64) for m_b = 2 and m_f =1, and minimizing the total potential energy Π with respect to the undetermined coefficient a and equating it to zero, after simplification, the dynamic stability formula is written, as

$$1-\frac{\left(\alpha\pm\frac{\beta}{2}\right)P_{cr}.4\frac{\pi^2}{L^2}}{\frac{\pi^4 EI}{L^4}\left[16+\frac{k_1L^4}{\pi^4EI}+\frac{4k_2L^2}{\pi^2EI}\right]}-\frac{\frac{\overline{m}\theta^2}{4}}{\frac{\pi^4EI}{L^4}\left[1+\frac{k_1L^4}{\pi^4EI}+\frac{k_2L^2}{\pi^2EI}\right]}=0 \qquad (3.79)$$

Substituting the corresponding reference values of $P_{cr}=\frac{4\pi^2EI}{L^2}$ and $\overline{m}=\frac{\pi^4EI}{\omega^2L^4}$ without considering the effect of the Pasternak foundation in Eq.(3.79) the value of Ω is

$$\Omega=\frac{\theta}{\omega}=2\sqrt{\left[\left((1-\alpha)(1\pm\mu)+\frac{\gamma_{F_1}}{16}+\frac{\gamma_{F_2}}{4}\right)\left(\frac{(1+\gamma_{F_1}+\gamma_{F_2})}{(1+\frac{\gamma_{F_1}}{16}+\frac{\gamma_{F_2}}{4})}\right)\right]} \qquad (3.80)$$

c) In the same way, substituting Eq.(3.23) in Eq.(3.64), and minimizing the total potential energy Π with respect to the undetermined coefficient *a* and equating it to zero, after simplification, for m_b = 2 and m_f = 2, the dynamic stability formula is

$$1-\frac{\left(\alpha\pm\frac{\beta}{2}\right)P_{cr}.4\frac{\pi^2}{L^2}}{\frac{\pi^4 EI}{L^4}\left[16+\frac{k_1L^4}{\pi^4EI}+\frac{4k_2L^2}{\pi^2EI}\right]}-\frac{\frac{\overline{m}\theta^2}{4}}{\frac{\pi^4EI}{L^4}\left[16+\frac{k_1L^4}{\pi^4EI}+\frac{4k_2L^2}{\pi^2EI}\right]}=0 \qquad (3.81)$$

Substituting the reference values, $P_{cr}=\frac{4\pi^2EI}{L^2}$ and $\overline{m}=\frac{16\pi^4EI}{\omega^2L^4}$ without considering the foundation, in Eq. (3.81) and after simplification, is written as

$$\Omega = \frac{\theta}{\omega} = 2\sqrt{(1-\alpha)(1\pm\mu) + \frac{\gamma_{F_1}}{16} + \frac{\gamma_{F_2}}{4}} \tag{3.82}$$

These three dynamic stability formulas i.e. Eqs.(3.78),(3.80) and (3.82) are derived based on the mode numbers m_b and m_f regardless the values of the first transition foundation parameter γ_{F_1} below or above the γ_{T1} (4).

3.3.2.1 General Dynamic Stability Formula

Interestingly, by substituting Eq.(3.23) in Eq.(3.65), and minimizing the total potential energy Π with respect to the undetermined coefficient a and equating it to zero, the reference critical load P_{cr} and frequency ω are with consideration of the Pasternak foundation, for one half sine wave for both the stability and vibration problems(m_b = m_f =1), when $\gamma_{F_1} < \gamma_{T1}$ and a full sine wave for both the stability and vibration problems (m_b = m_f =2) when $\gamma_{F_1} > \gamma_{T1}$, where the value of γ_{T1}= 4, after simplification, the general dynamic stability formula, obtained as

$$\Omega = \frac{\theta}{\omega} = 2\sqrt{(1-\alpha)(1\pm\mu)} \tag{3.83}$$

Use of these specific reference values of λ_b and λ_f the general dynamic stability curves turn out to be simple to use, exactly the same and are independent of the foundation parameters γ_{F_1} and γ_{F_2} for the same values of m_b and m_f (either 1 or 2). It may be noted here that the general dynamic stability formula presented in Eq. (3.83) does not contain the foundation parameters explicitly, unlike the three earlier formulas given in Eqs. (3.78),(3.80) and (3.82).

3.3.3 Numerical Results and Discussion

In the first three concise dynamic stability formulas (Eqs.(3.78),(3.80) and (3.82)) presented, the reference values used for the buckling load and the frequency parameters for the purpose of non-dimensionalization, correspond to the simply supported beam without considering the effect of the Pasternak foundation. Thus, three different sets of dynamic instability regions are obtained for the different values of the non–dimensional parameters μ and Ω. The mode shapes of the buckling do change when the values of γ_{F_1} considered is below or above the first transition foundation parameter γ_{T_1}. Free vibration mode shapes are invariant with respect to the values of γ_{F_1}. The value of γ_{F_2} does not contribute to the phenomenon of the transition of mode shapes for both the buckling and the vibration problems on the Pasternak foundation. Ultimately, the values of all the physical parameters involved will turn out to be the same if the non-dimensional quantities are converted to physical parameters. But the relative simplicity seen in these non-dimensional dynamic stability formulas will be lost while converting to represent these formulas to the dimensional forms, a multitude of dynamic stability curves are obtained, and are not easy to clearly demonstrate the actual behavior of the dynamic stability of simply supported beams, as the number of physical parameters involved are too many. The trend of the variation of λ_b and λ_f, with respect to the

foundation parameter and the mode numbers for the buckling and the free vibration, is as anticipated.

Table.3.13 gives the values of the buckling load λ_b and the frequency λ_f parameters for different values of γ_{F_1}, γ_{F_2}, m_b and m_f. Fig.3.3 shows the simply supported beam resting on a Pasternak foundation subjected to the end axial concentrated periodic loads. Fig.3.14 shows the dynamic stability curves for the instability boundaries $\Omega_1$and Ω_2, between which the simply supported beam is dynamically unstable, for varying μ, with the values of $m_b = m_f = 1$ for $\gamma_{F_1} = 2$ ($< \gamma_{T_1}$) and $\gamma_{F_2} = 0.1$. In this Fig. 3.14, and all the subsequent Figs. 3.15 to 3.23, the values of α considered are 0.0, 0.5 and 0.8. Fig.3.15 shows the similar curves as in Fig.3.14 with $\gamma_{F_2} = 0.2$ with the other non-dimensional parameters remaining the same. From these two figures it is seen that the change in the dynamic instability for $\gamma_{F_2} = 0.1$ and 0.2 is insignificant. The dynamic instability regions in terms of μ and Ω are shown in Figs.3.16 and 3.17 for the values of $\gamma_{F_1} = 3 (< \gamma_{T_1})$, $m_b = m_f = 1$ for both the buckling and the vibration problems for $\gamma_{F_2} = 0.1$ and 0.2 respectively. Again, it is observed from these figures that though the effect of γ_{F_1} is considerable, the effect of γ_{F_2} on the dynamic instability regions is negligible.

Figs.3.18 and 3.19 show the similar instability regions for γ_{F_1} = 4.5(> γ_{T_1}) for two values of γ_{F_2} = 0.1 and 0.2. The values of m_b and m_f are 2 and 1 respectively. The value of γ_{F_1} considered here is above the first transition foundation parameter γ_{T_1}, where the mode shape of buckling changes from 1 to 2 and the vibration mode shape remains the same at 1. Comparison of the dynamic instability regions presented in Figs.3.16 and 3.17, and Figs. 3.18 and 3.19 the value of γ_{F_1}(4.5) plays an important role on the dynamic stability regions. For a given μ the dynamic instability regions drastically increase from γ_{F_1} = 3 to γ_{F_1} = 4.5. As observed earlier, the effect of the second foundation parameter on these regions is insignificant whether the value is 0.1 or 0.2.

Figs. 3.20 and 3.21 show a similar trend as observed in Figs.3.18 and 3.19, where γ_{F_1} = 5.5(> γ_{T_1}), the values of m_b and m_f are 2 and 1 respectively. A change in the instability regions for the earlier two figures given for γ_{F_1} = 4.5 and from the present set of figures can be visually seen and the effect of γ_{F_2} is negligible.

The dynamic instability regions for the values of γ_{F_1} = 5.5(> γ_{T_1}) with m_b= m_f = 2 and for the value of γ_{F_2} = 0.1 and 0.2 are shown in Figs.3.22

and 3.23. It is observed that for these values of γ_{F_1} and γ_{F_2} there isn't any impact on the dynamic instability regions.

In all the Figs. 3.14 to 3.23, the values of γ_{T_1} is the first transition value and is equal to 4. The reference values of P_{cr} and ω taken are without considering the Pasternak foundation, Viz., $\gamma_{F_1} = \gamma_{F_2} = 0$ and $m_b = m_f = 1$ (Table 3.13).

Finally, the dynamic instability regions for $m_b = m_f = 1$ for the value of the foundation parameter γ_{F_1} below the first transition value $\left(\gamma_{F_1} < \gamma_{T_1}\right)$ and $m_b = m_f = 2$ in both the stability and vibration problems, for the first foundation parameter above the first transition value $\left(\gamma_{F_1} > \gamma_{T_1}\right)$ using Eq. (3.83) are shown in Fig.3.7. The reference values of the buckling load and the frequency parameters used here are obtained by considering the effect of the Pasternak foundation. With these non-dimensionalization all the earlier discussed dynamic instability boundaries collapse into a single dynamic instability boundary for a given α and varies with α only with respect to μ and Ω. These curves obtained for different α_s are named as general dynamic stability curves and shown in Fig. 3.7. It is emphasized here that this generality, shown in the general dynamic instability boundaries, with rigorous explanation, is not recognized in the earlier studies of the researchers, on this topic.

3.4 DYNAMIC STABILITY OF BEAMS SUBJECTED TO END PERIODIC AND STATIC TENSILE AXIAL LOADS

With the background gained from the literature, the dynamic stability of beams subjected to end periodic and static tensile axial loads is studied in this section. The Euler-Bernoulli beam is considered to study the dynamic instability boundaries. It is to be noted here that the study on beams, irrespective of the boundary conditions and the stability regions of the dynamic stability problem can be obtained, using single term trigonometric admissible functions.

In all the earlier studies on this topic, dynamic stability prediction, the static axial load is taken as compressive. In this section, to study the dynamic stability behavior for the beams subjected to the combination of two types of concentrated loads, namely, end axial periodic and constant tensile static loads.

3.4.1 Formulation

The energy method (RR method) is used in the present section to evaluate the dynamic stability regions of the uniform slender beams subjected to an end periodic and a tensile static load. A beam of length L, subjected to a concentrated end axial periodic load *P(t)*, is shown in Fig.3.4. The total potential energy Π, of the beam is given by

$$\prod = U - T - W \tag{3.84}$$

where *U, T* and *W* are the strain energy, kinetic energy and potential due to work.

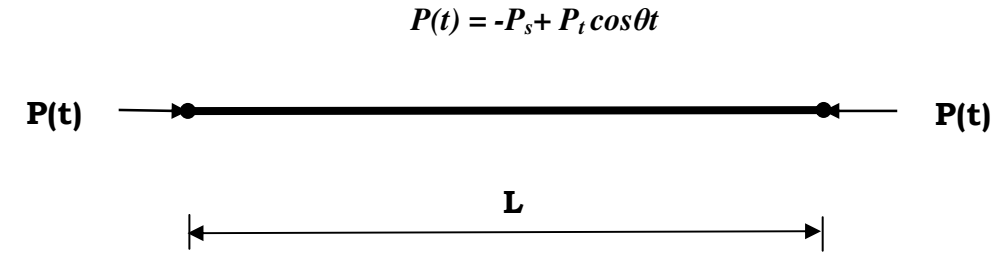

Fig.3.4 Uniform beam subjected to end axial periodic load

The periodic load P *(t)* is taken as

$$P(t) = -P_S + P_t \cos\theta t \tag{3.85}$$

The quantities P_s and P_t are expressed in terms of the critical load P_{cr}, where the negative sign indicates that the static load P_s is tensile.

Substituting, the energy expressions and potential due to work, in Eq.(3.84), the energy equation governing the dynamic stability problem of the beams is written as

$$\Pi = \frac{EI}{2}\int_0^L w''^2 dx - \frac{P(t)}{2}\int_0^L w'^2 dx - \frac{\overline{m}\,\omega^2}{2}\int_0^L w^2 dx \tag{3.86}$$

Eq. (3.86) becomes

$$\Pi = \frac{EI}{2}\int_0^L w''^2 dx - \frac{P(t)}{2}\int_0^L w'^2 dx - \frac{\overline{m}}{2}\frac{\theta^2}{4}\int_0^L w^2 dx \tag{3.87}$$

Substituting the expression for *P (t)* given in Eq. (3.85) in Eq.(3.87), we get

$$\Pi = \frac{EI}{2}\int_0^L w''^2 dx - \left(-P_S + P_t \cos\theta t\right)\frac{1}{2}\int_0^L w'^2 dx - \frac{\overline{m}}{2}\frac{\theta^2}{4}\int_0^L w^2 dx \qquad (3.88)$$

or

$$\Pi = \frac{EI}{2}\int_0^L w''^2 dx - \frac{(-P_s)}{2}\int_0^L w'^2 dx - (p_t \cos\theta t)\frac{1}{2}\int_0^L w'^2 dx - \frac{\overline{m}}{2}\frac{\theta^2}{4}\int_0^L w^2 dx \qquad (3.89)$$

As a first approximation solution [17], the condition for the existence of these boundary solutions is

$$\Pi = \frac{EI}{2}\int_0^L w''^2 dx - \frac{(-\alpha P_{cr})}{2}\int_0^L w'^2 dx - \frac{(\pm\beta P_{cr})}{2}\frac{1}{2}\int_0^L w'^2 dx - \frac{\overline{m}}{2}\frac{\theta^2}{4}\int_0^L w^2 dx \qquad (3.90)$$

In this analysis, the static buckling load parameter λ_b of the beam is considered as the reference load for the purpose of non-dimensionalization. Further analysis is presented in detail for the boundary conditions of the beam as follows.

3.4.1.1 Simply supported beam:

For simply supported beam, the lateral deflection, assumed as single term standard exact trigonometric admissible function in the non--dimensional form, as given in Eq. (3.23), is

$$\overline{w} = a\sin\pi\overline{x}$$

Non-dimensionalizing the Eq. (3.90), all the length quantities with respect to the length of the beam *L*, we get

$$\Pi = \frac{EI}{2L}\int_0^1 \overline{w}''^2 d\overline{x} - \frac{(-\alpha P_{cr})L}{2}\int_0^1 \overline{w}'^2 d\overline{x} - \frac{(\pm\beta P_{cr})L}{2}\frac{1}{2}\int_0^1 \overline{w}'^2 d\overline{x} - \frac{\overline{m}}{2}\frac{\theta^2 L^3}{4}\int_0^1 \overline{w}^2 d\overline{x} \quad (3.91)$$

For the degenerate case of the free vibration problem of the initially loaded beam with the constant axial tensile load (P_s = -α P_{cr}, consistent with the sign convention used for the applied load) and without the periodic part of the load (β = 0), Eq. (3.91) becomes

$$\Pi = \left(\frac{EI}{2L} \int_0^1 \overline{w}''^2 d\overline{x} - \frac{(-\alpha) P_{cr} L}{2} \int_0^1 \overline{w}'^2 d\overline{x} \right) - \frac{\overline{m}\,\omega^2}{2} L^3 \int_0^1 \overline{w}^2 d\overline{x} \tag{3.92}$$

and in Eq. (3.92) the potential due to work with the axial tensile static load is combined with the strain energy expression, this implies the stiffness of the beam is altered (increased) with the initial axial tensile load.

Substituting, Eq. (3.23) in Eq. (3.92) and minimizing the total potential energy Π with respect to the undetermined coefficient a, and equating it to zero, for the first mode, after simplification, the frequency parameter of beam with the initial tensile load αP_{cr} as

$$\lambda_f = \frac{\overline{m}\,\omega^2 L^4}{EI} = \pi^4 \left[1 - (-\alpha) \right] \tag{3.93}$$

Here, the value of the frequency parameter is obtained including the initial tensile load.

Substituting, Eqs. (3.23) in (3.91), and minimizing the total potential energy Π with respect to the undetermined coefficient a, and equating it to zero, for the first mode, after simplification, the dynamic stability equation is expressed as

$$1-(-\alpha)\mp\frac{\beta}{2}-\frac{\theta^2}{4\omega^2}\left[1-(-\alpha)\right]=0 \tag{3.94}$$

Equation (3.94) becomes

$$1\mp\frac{\beta}{2\left[1-(-\alpha)\right]}-\frac{\Omega^2}{4}=0 \tag{3.95}$$

Equation (3.95) is further simplified as

$$\Omega=2\sqrt{\left(1\mp\frac{\beta}{2\left[1-(-\alpha)\right]}\right)} \tag{3.96}$$

Using Eq. (3.96), the dynamic stability regions are obtained for a given α, from which the dynamic instability boundaries can be obtained in terms of the simple non-dimensional physical parameters Ω and β.

Hence, Eq. (3.96) can be treated as the general dynamic stability solution containing the simple physically identifiable non-dimensional parameters. On the other hand, the general dynamic stability solution presented in earlier sections is from an abstract non-dimensional parameter μ used by many researchers, along with Ω.

3.4.1.2 Clamped beam:

Using the non-dimensional parameters, for the clamped-clamped beam, the distribution of the lateral deflection $\overline{w}$ is assumed as

$$\overline{w}=a(1-\cos 2\pi\bar{x}) \tag{3.97}$$

Substituting the Eq. (3.97) in Eq. (3.92), and minimizing the total potential energy Π with respect to the undetermined coefficient *a*, and

equating it to zero, after simplification, for the clamped-clamped beam with the initial tensile load, the frequency parameter, is obtained as

$$\lambda_f = \frac{\overline{m}\,\omega^2 L^4}{EI} = \frac{16}{3}\pi^4\left[1-(-\alpha)\right] \tag{3.98}$$

Substituting Eq. (3.97) in Eq. (3.91), and minimizing the total potential energy Π with respect to the undetermined coefficient a, and equating it to zero, for the first mode of vibration and buckling, after simplification, the dynamic stability equation is obtained for the clamped beam, is the same as that given in Eq. (3.96), from which the dynamic instability regions can be evaluated.

3.4.1.3 Cantilever beam (C-F):

Using the non-dimensional parameters, for the clamped-free beam, the distribution of the lateral deflection $\overline{w}$ is assumed as

$$\overline{w} = a(1-\cos\frac{\pi\bar{x}}{2}) \tag{3.99}$$

Substituting the Eq. (3.99) in Eq. (3.92), and minimizing the total potential energy Π with respect to the undetermined coefficient a and equating it to zero, after simplification, for the clamped- free beam with the initial tensile load, the frequency parameter, is obtained as

$$\lambda_f = \frac{\overline{m}\,\omega^2 L^4}{EI} = \frac{\pi^4\left[1-(-\alpha)\right]}{\left(48-\frac{128}{\pi}\right)} \tag{3.100}$$

Substituting Eq. (3.99) in Eq.(3.91), and minimizing the total potential energy Π with respect to the undetermined coefficient *a*, and equating it to zero, for the first mode of vibration and buckling, after simplification, the dynamic stability equation is obtained for the cantilever beam, is the same as that given in Eq. (3.96), from which the dynamic instability regions can be evaluated.

3.4.1.4 Clamped- simply supported beam(C-S):

Using the non-dimensional parameters, for the clamped-hinged beam, the distribution of the lateral deflection $\overline{w}$ is taken as

$$\overline{w} = a(\cos\frac{3\pi\overline{x}}{2} - \cos\frac{\pi\overline{x}}{2}) \tag{3.101}$$

Substituting the Eq. (3.101) in Eq. (3.92), and minimizing the total potential energy Π with respect to the undetermined coefficient *a*, and equating it to zero, after simplification, for the clamped- simply supported beam with the initial tensile load, the frequency parameter, is obtained as

$$\lambda_f = \frac{\overline{m}\,\omega^2 L^4}{EI} = \frac{41}{16}\pi^4\left[1-(-\alpha)\right] \tag{3.102}$$

Substituting, Eq. (3.101) in Eq. (3.91), and minimizing the total potential energy Π with respect to the undetermined coefficient *a*, and equating it to zero, for the first mode of vibration and buckling, after simplification, the dynamic stability equation is obtained for the clamped-simply

supported beam, is the same as that given in Eq. (3.96), from which the dynamic instability regions can be evaluated.

A close observation of Eq. (3.96) shows that the dynamic instability regions, for the above boundary conditions of the beam, will be the same if the same non-dimensional parameters for the lateral deflection and the axial coordinate are used. Hence, Eq. (3.96) can be treated as the general dynamic stability solution containing the simple physically identifiable non-dimensional parameters. On the other hand, the general dynamic stability solution given in Eq. (3.30) of section 3.1 is from an abstract non-dimensional parameter μ $\left(=\frac{\beta}{2(1-\alpha)}\right)$ along with Ω.

In this section the buckling load parameter is defined, as

$$\lambda_b = \frac{P_{cr} L^2}{EI} \tag{3.103}$$

and is evaluated by minimizing the total potential energy Π, where

$$\Pi = \frac{EI}{2}\int_0^L w''^2 dx - \frac{P_s}{2}\int_0^L w'^2 dx \tag{3.104}$$

with the value of $P_t = 0$.

Substituting, the lateral deflection w in Eq.(3.104), and minimizing the total potential energy Π with respect to the undetermined coefficient a, and equating it to zero, for the first mode of the buckling, and after simplification. The value of λ_b is π^2, $4\pi^2$, $\pi^2/4$ and $41\pi^2/20$ for the simply

supported, clamped-clamped, clamped-free and clamped-simply supported beams respectively.

It is to be noted here that, the value of the radian frequency parameter of the beam is obtained considering the effect of initial tensile load P_s in the evaluation of the strain energy. The general dynamic stability formula derived in Eq.(3.30) of section 3.1, is obtained using the radian frequency parameter, without considering the constant axial load (P_s). This procedure gives the following equations with the same notation followed in this work from which the solution for the dynamic stability problem of the beam for any boundary condition is obtained, the equation being

$$1-\left(-\alpha \pm \frac{\beta}{2}\right)-\frac{\Omega^2}{4}=0 \tag{3.105}$$

Equation (3.105) is further simplified as

$$\Omega = 2\sqrt{(1-(-\alpha)(1\pm\mu))} \tag{3.106}$$

Using Eq. (3.106), the dynamic stability regions can be obtained for a given α, in terms of Ω and μ. The detailed derivation of these equations is not presented here for the sake of brevity and can be seen in section 3.1.

3.4.2 Numerical Results and Discussion

Fig.3.4 shows a uniform beam subjected to the periodic and tensile static axial loads. An alternate general dynamic stability formula, that uses the non dimensional parameters β and Ω, is derived in this section,

to predict the dynamic stability analysis of beams, subjected to the combination of the axial periodic and constant tensile static axial loads, applicable for any boundary condition of the beam. In the non-dimensional form, the characteristic values of the beam, such as the fundamental radian frequency and the static buckling load parameters, do not appear explicitly. However, these characteristic values appear implicitly in the definition of the non-dimensional parameters α, β, Ω and μ defined earlier.

Table 3.24 gives the values of the stability boundaries Ω_1 and Ω_2, evaluated using the first mode of the stability and vibration, with varying β, for α = 0.0, 0.5, 1.0 and 4.0 (tensile), between which the beam is dynamically unstable. In Fig.3.24, the corresponding dynamic stability curves are presented. It is observed that the value of dynamic instability starts with the value of 2.0 for all the values of α considered and the instability regions are decreasing for the higher values of the tensile static load parameter. The curves presented in this Fig.3.24 clearly, and without any ambiguity, show the physical trend that the tensile static load has a stabilizing effect on the dynamic stability behavior.

Table 3.25 and Fig. 3.25 shows the dynamic stability curves for the same beam problem considered in section 3.1. It is observed that, the regions of dynamic stability seems to be increasing with increasing tensile static load parameter and may give a seemingly wrong

interpretation to the readership. The reason for this anomalous behavior is the use of different non-dimensional parameters, the physically recognizable non-dimensional parameter β compared to the abstract non-dimensional parameter μ in the present and earlier studies respectively. However, it may be noted here that the Figs. 3.24 and 3.25 are mutually convertible to each other by a proper manipulation on the non-dimensional parameters used.

3.5 DYNAMIC STABILITY OF TAPERED BEAM SUBJECTED TO END CONCENTRATED AXIAL PERIODIC LOADS

With the background gained from the literature, the dynamic stability of simply supported tapered beam subjected to concentrated end axial periodic loads P(t), is studied in this section.

A tapered simply supported beam of Length *L*, Young's modulus *E* and mass per unit length $\overline{m}$ as shown in Fig.3.5,

The variations of area of cross section of the beam A_b and moment of inertia *I* are given by

$$A_b = \begin{Bmatrix} A_c\left[1-\bar{d}+(2x/L)\bar{d}\right]^{n_1} for 0 \le x \le L/2 \\ A_c\left[1+\bar{d}-(2x/L)\bar{d}\right]^{n_1} for L/2 \le x \le L \end{Bmatrix} \tag{3.107}$$

$$I = \begin{Bmatrix} I_c\left[1-\bar{d}+(2x/L)\bar{d}\right]^{n_2} for 0 \le x \le L/2 \\ I_c\left[1+\bar{d}-(2x/L)\bar{d}\right]^{n_2} for L/2 \ge x \ge L \end{Bmatrix} \tag{3.108}$$

where A_c is the area of the cross-section and I_c is the area moment of Inertia at the mid point of the beam respectively, and x is the axial co-ordinate as shown in Fig.3.5, $\bar{d}\left(=\frac{D_1-D_2}{D_1}\right)$ is the taper parameter, D_1 and D_2 are the depths or diameters of the beam at the centre (midpoint) and ends of the beam respectively, depth is considered to vary linearly while the breadth is maintained as uniform as shown in Fig.3.5.

In Eqs.(3.107) and (3.108) the values of the n_1 and n_2 are n_1=1and n_2=3 for depth taper, and n_1 = 2 and n_2=4 for diameter taper.

3.5.1 Dynamic Stability Formula

When the tapered simply supported beam, subjected to an axial periodic loads P(t), as given in Eq.(3.2), the instability regions, can be obtained from the solution of approximate continuum method or the numerical methods, solving the following matrix equation of equilibrium, derived by Bolotin [17], as

$$[K]\{\delta\}-\left(P_s \pm \frac{P_t}{2}\right)[G]\{\delta\}-\frac{\theta^2}{4}[M]\{\delta\}=0 \qquad (3.109)$$

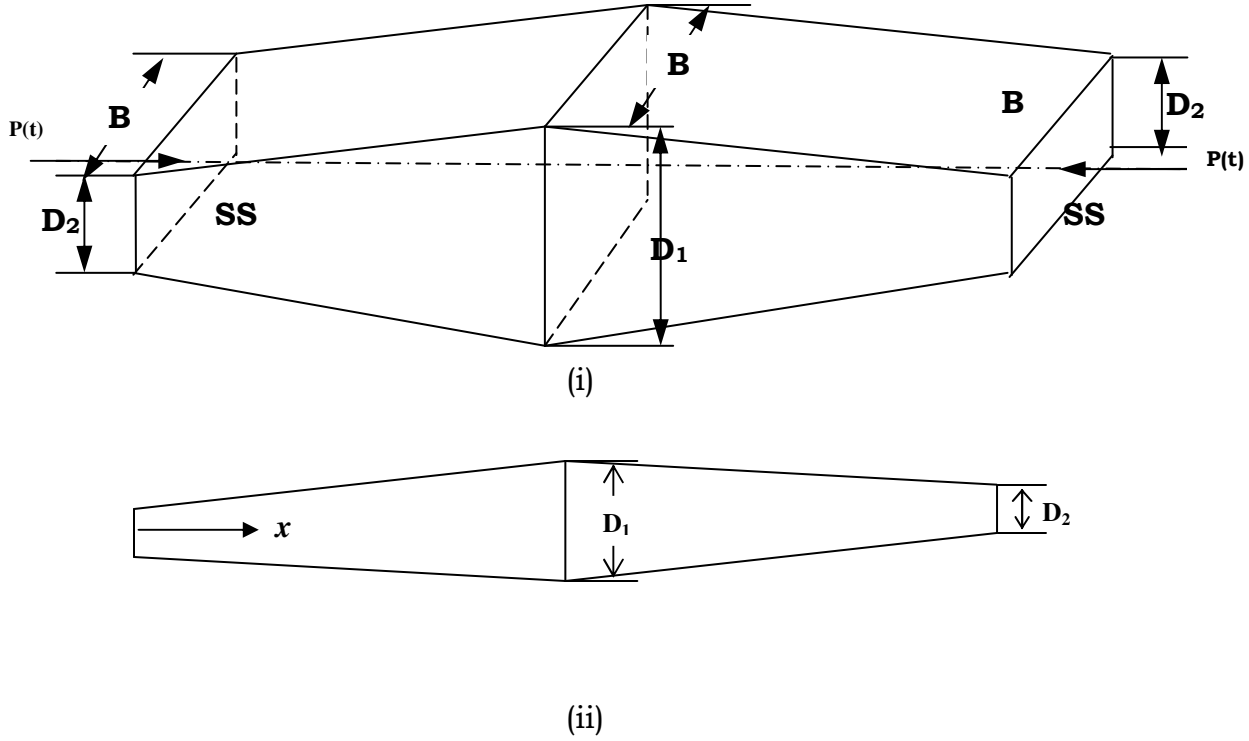

Geometry of tapered beams (i) Depth taper (ii) Diameter taper

Fig. 3.5 A simply supported tapered beam subjected to end concentrated periodic loads.

where [K], [G] and [M] are the system stiffness matrix, system geometric stiffness matrix and system mass matrix respectively and {δ} is the eigenvector.

Many researchers presented in their new studies on the dynamic stability of different structural members starting from this standard matrix equation. These matrices represent explicitly for a specific structural member and hence, this equation is valid for any structural member. A detailed derivation of this equation is well documented in the classic work of Bolotin [17], and the main objective of the study in this section is

to derive a dynamic stability formula for a tapered beam, which is presented in this section in the form of this matrix equation.

From Eq. (3.109), the governing equation for the vibration problem can be written, neglecting the load term, as

$$[K]\{\delta_1\}-\omega_{NU}{}^2[M]\{\delta_1\}=0 \tag{3.110}$$

Equation (3.110) can be rewritten as

$$[M]\{\delta_1\}=\frac{1}{\omega_{NU}{}^2}[K]\{\delta_1\} \tag{3.111}$$

Subscript $_{NU}$ denotes non uniform, where ω_{NU} is the natural frequency of tapered (non uniform) beam.

Similarly, by neglecting the inertia term, the solution of the buckling problem in terms of the buckling load can be obtained from the degenerate case of Eq. (3.109), as

$$[K]\{\delta_2\}-P_{crNU}[G]\{\delta_2\}=0 \tag{3.112}$$

or

$$[G]\{\delta_2\}=\frac{1}{P_{crNU}}[K]\{\delta_2\} \tag{3.113}$$

where P_{crNU} is the critical load of a tapered(non uniform) beam.

Here, a reasonable assumption for the first mode which is valid for most of the structural members can be made as

$$\{\delta_1\}=\{\delta_2\}=\{\delta\} \tag{3.114}$$

Substituting, the Eqs. (3.111), (3.113) and Eq. (3.114) in Eq. (3.109), we get

$$[K]\{\delta\}-(P_s \pm \frac{P_t}{2})\frac{1}{P_{crNU}}[K]\{\delta\}-\frac{\theta^2}{4}\frac{1}{\omega_{NU}{}^2}[K]\{\delta\}=0 \tag{3.115}$$

or

$$[K]\{\delta\}-(\alpha \pm \beta/2)[K]\{\delta\}-\frac{\theta^2}{4\omega_{NU}{}^2}[K]\{\delta\}=0 \tag{3.116}$$

where $\alpha=\frac{P_s}{P_{crNU}}$ and $\beta=\frac{P_t}{P_{crNU}}$

Equation (3.116), written as

$$\frac{\theta^2}{4\omega_{NU}{}^2}=(1-\alpha)(1\pm\mu) \tag{3.117}$$

Hence, the ratios of

$$\frac{\theta}{\omega_{NU}}=\Omega_{NU}=2\sqrt{(1-\alpha)(1\pm\mu)} \tag{3.118}$$

where Ω_{NU} and μ are the non-dimensional parameters used by Brown *et al.* [18]. It is seen from the Eq.(3.118) that these non-dimensional parameters are independent of the characteristic values of the ω_{NU} and P_{crNU} of the tapered beam considered and it can be used as a general dynamic stability formula as it is the most general form and is invariant for the beam configuration. However, to obtain the absolute values of the dynamic stability boundaries of a tapered beam the corresponding values of ω_{NU} and P_{crNU} have to be used. Evaluation of these values or quantities is a standard procedure, which can be obtained from the literature [33].

3.5.2 Numerical Results and Discussion

Fig.3.5 shows the geometry of the tapered, homogeneous beam subjected to concentrated end axial periodic loads. The numerical values of the instability regions are obtained using the formula, derrived in the present section, in terms of the non-dimensional parameters μ and $\Omega_{NU}\left(=\frac{\theta}{\omega_{NU}}\right)$.

Table 3.4 gives the dynamic stability regions, with reference to the nondimensional quantities μ, Ω_{NU} and α, of the tapered beam. It can be verified that the formula developed in this section of Eq. (3.118) is exactly the same as that derived in Eq.(3.30) of the section 3.1, applicable for the uniform beams, by virtue of the use of the suitable non dimensional parameters in both the studies. The numerical values given in Table 3.4 brings out the important point that the dynamic instability regions are invariant with beam configuration.

In the nondimensional form the characteristic values of the beam such as the fundamental frequency and the buckling load parameters do not appear explicitly. However these characteristic values are appearing implicitly in the definition of μ and Ω.

3.6 DYNAMIC STABILITY OF SQUARE PLATE SUBJECTED TO A COMBINATION OF CONSTANT AND PERIODIC LOADS

In this section, the dynamic stability behavior of the square plate subjected to uniform edge in-plane periodic loads, consisting of a constant compressive and periodic load in one direction and constant compressive load in the perpendicular direction, as shown in Fig.3.5a, is investigated. The simply supported boundary conditions with varying uniform constant compressive load ratios are considered in this study. In this work an energy method is used to develop a simple closed form solution to predict the dynamic stability behavior of the simply supported square plate, using the exact trigonometric admissible function to represent the lateral deflection. Leissa [88] compiled the several free vibration formulations and corresponding results are presented in a systematic way.

It is the endeavor of the researcher to develop simple solutions, to some complex problems of practical interest in the structural mechanics, and successfully developed proper formulations to predict the fundamental frequency parameters of structural members in the works of [35, 42, 47, 84, 88, 92 and 93]. In the same spirit, a simple formula is successfully developed to predict the dynamic stability boundaries of the square plate subjected to the aforementioned loads. It is to be noted here that the prediction of dynamic stability behavior of the plate with these

applied loads is a new study to analyze the dynamic stability behavior of square plate. In the following section, the simple formula to predict the dynamic stability behavior of the simply supported square plate subjected to the loading condition mentioned earlier is presented.

3.6.1 Formulation

When the plate is subjected to a uniform in-plane periodic load in the x- direction and a constant compressive load in the y- direction, as shown in Fig.3.5a, the periodic load $N_x(t)$ and N_y, which are defined as,

$$N_x(t) = N_s + N_t \cos \theta t = (\alpha \pm \beta \cos \theta t) N_{cr} \tag{3.119}$$

and

$$N_y = L_R N_x \tag{3.120}$$

Where α is the static load factor$\left(= \frac{N_s}{N_{cr}}\right)$, β is the dynamic load factor$\left(= \frac{N_s}{N_{cr}}\right)$, N_s is the constant compressive load, N_t is the time dependent load, N_{cr} is the critical load, θ is the applied radian frequency, t is the time and $L_R = \frac{N_x}{N_y}$.

A plate of length *A* and breadth *B* with constant thickness *h*, the strain energy U, the potential due to work *W* and the kinetic energy *T* are given by

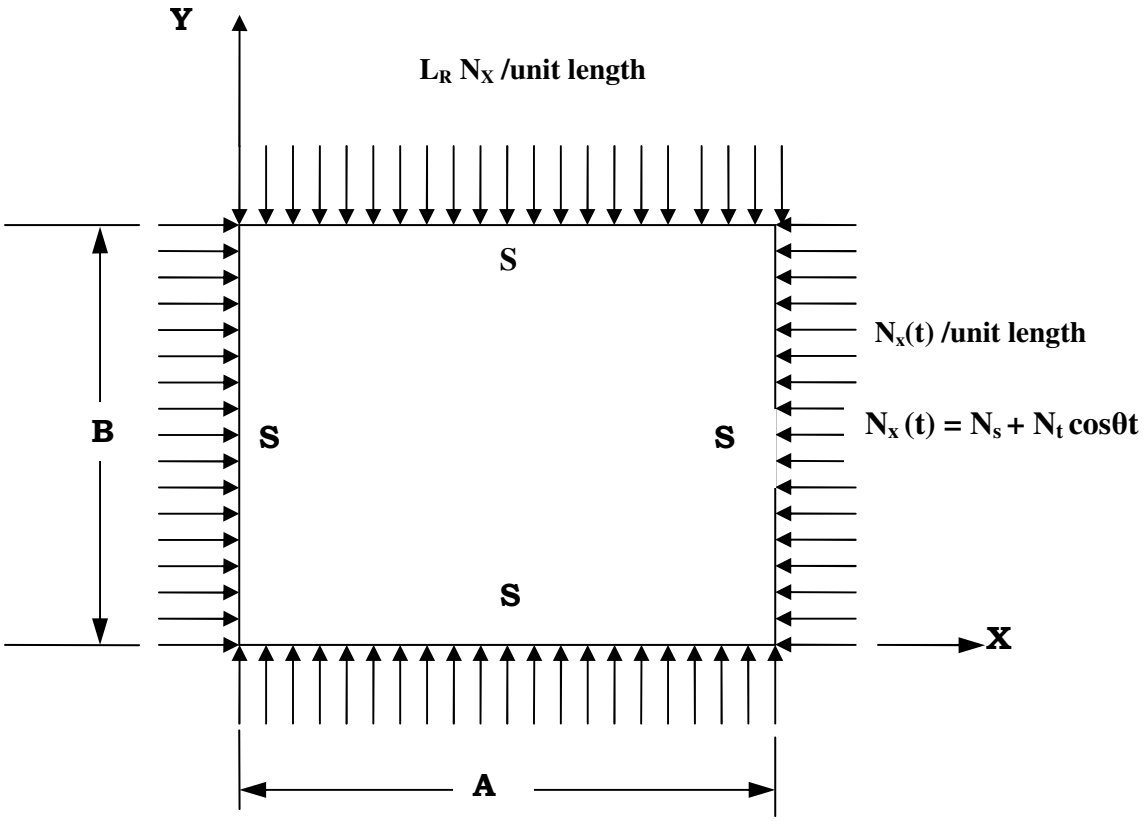

Fig. 3. 5a. A simply supported plate under the applied compressive load system

$$U = \frac{D}{2}\int_0^B\int_0^A \left[\kappa_x^2 + \kappa_y^2 + 2\nu\kappa_x\kappa_y + \frac{1-\nu}{2}\kappa_{xy}^2 \right] dxdy \qquad (3.121)$$

$$W = \frac{N_x(t)}{2}\int_0^B\int_0^A \left(\frac{\partial w}{\partial x}\right)^2 dxdy + \frac{L_R N_x}{2}\int_0^B\int_0^A \left(\frac{\partial w}{\partial y}\right)^2 dxdy \qquad (3.122)$$

and

$$T = \frac{\rho t\omega^2}{2}\int_0^B\int_0^A w^2 dxdy \qquad (3.123)$$

with

$$\kappa_x = -\frac{\partial^2 w}{\partial x^2}, \kappa_y = -\frac{\partial^2 w}{\partial y^2}, \quad \kappa_{xy} = -2\frac{\partial^2 w}{\partial x \partial y} \qquad (3.124)$$

where w is the lateral displacement, ρ is the mass density, ω is the radian frequency, $N_x(t)$ and N_y are the edge uniform periodic and constant compressive loads in the Cartesian x and y co-ordinate directions respectively, and D is the plate flexural rigidity given by $D = \frac{Eh^3}{12(1-\nu^2)}$, E is the young's modulus, h is the thickness of the plate and ν is the Poisson ratio.

The lateral displacement w in terms of m and n, the number of half sine waves in x and y directions respectively, is assumed to be of the form,

$$w = a\sin\left(\frac{m\pi x}{A}\right)\sin\left(\frac{n\pi y}{B}\right) \qquad (3.125)$$

where a is the undetermined coefficient.

The displacement distribution assumed for w is exact for the simply supported boundary conditions.

The total potential energy Π of the plate is given by

$$\Pi = U - W - T$$

where U, T and W are the strain energy, kinetic energy and potential due to work respectively.

In the Rayleigh-Ritz method, the total potential energy is minimized with respect to the undetermined coefficient a, as

$$\frac{\partial \Pi}{\partial a} = \left(\frac{\partial}{\partial a}\right)(U - W - T) = 0 \qquad (3.126)$$

which yields, after integration and simplification of Eq.(3.126)by neglecting W, an expression for frequency parameter, λ_f $(=\frac{\rho h \omega^2 A^4}{D})$ is obtained as

$$\lambda_f = \pi^4 \left(m^2 + n^2 \frac{A^2}{B^2} \right)^2 \tag{3.127}$$

Similarly, by neglecting the kinetic energy T in Eq.(3.126), the expression for the buckling load parameter, λ_b $(=\frac{N_{xcr} A^2}{\pi^2 D}$, where N_{xcr} is the critical load in x-coordinate) is obtained as

$$\lambda_b = \frac{\left(m^2 + n^2 \frac{A^2}{B^2} \right)^2}{\left(m^2 + L_R n^2 \frac{A^2}{B^2} \right)} \tag{3.128}$$

Substituting, the energies U and T and potential W in Eq. (3.126), after simplification, using the Eqs.(3.127) and Eq.(3.128), the dynamic stability equation in the non-dimensional form, as

$$1 - \frac{\left\{ \left(\alpha \pm \frac{\beta}{2} \right) m^2 + L_R n^2 \frac{A^2}{B^2} \right\}}{\left(m^2 + L_R n^2 \frac{A^2}{B^2} \right)} - \frac{\theta^2}{4\omega^2} = 0 \tag{3.129}$$

For a square plate (A/B =1), for the first mode of buckling and vibration (m = n = 1), Eq. (3.129) becomes

$$1 - \frac{\left\{ \left(\alpha \pm \frac{\beta}{2} \right) + L_R \right\}}{\left(1 + L_R \right)} - \frac{\theta^2}{4\omega^2} = 0 \tag{3.130}$$

Defining, $\Omega = \frac{\theta}{\omega}$ and after simplification, Eq. (3.130) becomes

$$\Omega = \frac{\theta}{\omega} = 2\sqrt{\frac{\left(1-\alpha \pm \frac{\beta}{2}\right)}{\left(1+L_R\right)}} \tag{3.131}$$

Equation (3.131) is rewritten as

$$\Omega = \frac{\theta}{\omega} = 2\sqrt{\frac{(1-\alpha)(1\pm\mu)}{\left(1+L_R\right)}} \tag{3.132}$$

where $\mu = \frac{\beta}{2(1-\alpha)}$

Using Eq. (3.132), the dynamic stability regions can be obtained for a given α, in terms of Ω and μ for different values of constant compressive load ratio (L_R), where Ω, μ and α are defined earlier.

Equation (3.131) can be treated as the dynamic stability solution containing the physically identifiable non-dimensional parameter (β). On the other hand, the dynamic stability solution presented in Eq. (3.132) contains an abstract non-dimensional parameter μ used by many researchers along with Ω and α.

3.6.2 Numerical Results and Discussion

Using, the Eqs. (3.131) and (3.132), the effect of the present in-plane loads considered as shown in Fig.3.5a, is brought out. Table 3.26 shows the variation of Ω_1 and Ω_2 for the value of β (dynamic load factor)

varying from 0 to 1.0 for the simply supported square plate with uniform uniaxial in-plane periodic load i.e. (L_R = 0.0) for α = 0.0, 0.25 and 0.5. The dynamic stability regions of the square plate are given in Ramachandra and Sarat Kumar [93] and the present results for L_R = 0.0 (Uniform uniaxial periodic loads) are deduced from the dynamic stability formula for α = 0.0 and 0.6 are given in Tables 3.27 and 3.28 respectively. The excellent agreement between the two results indicates the usefulness of the simple formula developed in the present work.

In Tables 3.29 and 3.30 the dynamic stability regions for the uniform biaxial load for L_R = 0.5 and 1 and α = 0.0, 0.25 and 0.5 in terms of Ω and β. One can observe that, by increasing of the static compressive load factor α, the width of the dynamic instability regions increase and by increasing the static compressive load ratio (L_R) the regions of the dynamic instability decreases and shifts towards the vertical axis.

The effect of load ratio L_R on the dynamic stability boundaries of a square plate is also presented here. It is observed that the buckling load decreases with increasing L_R form 0 to1. Table 3.31 shows the variation of Ω_1 and Ω_2 with respect to abstract non-dimensional parameter (μ) for the simply supported plate with uniaxial in-plane periodic load, when L_R = 0 for α = 0.0, 0.5 and 0.8. Graphical representation of these results is shown in Fig. 3.29. It is seen from the Table 3.31 and Fig. 3.29 that

these are same as the general dynamic stability results presented in the digital and analogue forms given in section 3.1.

Table 3.32 and 3.33 shows the variation of Ω_1 and Ω_2 with μ for the simply supported plate with constant compressive load ratio, L_R = 0.5 and 1 for α = 0.0, 0.5 and 0.8 respectively. One can observe from the Tables 3.31 to 3.33 and Figs.3.29 to 3.31 that by increasing the static load factor α width of the dynamic instability regions decrease and by increasing the constant compressive static load ratio(L_R) the regions of dynamic instability decrease and shift towards the vertical axis.

3.7 CONCLUDING REMARKS

In this chapter, a general dynamic stability formula is developed for the beams and plates. The condition that, the mode shapes of fundamental frequency and buckling are the similar is satisfied exactly by choosing appropriate accurate single term admissible functions. Finally, it is concluded based on the numerical results obtained that the formula developed in this chapter can be used as a general dynamic stability formula applicable for beams including the secondary effects like the elastic foundation and tapered configurations and a plate. This is due to the non dimensional parameters used, for the periodic loads and the applied radian frequency with the use of reference values (P_{REF} and ω_{REF}) corresponding to the actual configuration of the beams and plates.

Table 3.1 Buckling load parameter λ_b and fundamental frequency parameter λ_f for the beam with various boundary conditions.

Boundary condition	**Type of admissible function**	**Lateral deflection 'w'**	$\lambda_b\left(=\frac{P_{cr}L^2}{EI}\right)$	$\lambda_f\left(=\frac{\overline{m}\omega^2L^4}{EI}\right)$
S-S	Trigonometric	$w = a\sin\frac{\pi x}{L}$	π^2	π^4
C-C	Trigonometric	$w=a\left(1-\cos\frac{2\pi x}{L}\right)$	$4\pi^2$	$\frac{16\pi^4}{3}$
C-F	Trigonometric	$w=a\left(1-\cos\frac{\pi x}{2L}\right)$	$\frac{\pi^2}{4}$	$\frac{\pi^4}{\left(48-\frac{128}{\pi}\right)}$
C-S	Trigonometric	$w=a\left(\cos\frac{3\pi x}{2L}-\cos\frac{\pi x}{2L}\right)$	$\frac{41\pi^2}{20}$	$\frac{41\pi^4}{16}$

Table 3.2 Comparison of the mode shapes of the L_2 norm of analytical and finite element solution for uniform beams

	Buckling (FE)	Vibration (FE)	Analytical function
16 elements			
S-S	2.8285	2.8285	2.8285
C-C	2.4494	2.5185	2.4494
C-H	2.6218	2.6564	2.6035
C-F	2.0357	2.1246	2.0357
32 elements			
S-S	4.0000	4.0000	4.0000
C-C	3.4642	3.5618	3.4642
C-H	3.6945	3.7524	3.6797
C-F	2.7864	2.9166	2.7864
64 elements			
S-S	5.6568	5.6568	5.6568
C-C	4.8992	5.0375	4.8992
C-H	5.2248	5.3011	5.1963
C-F	3.8751	4.0625	3.8751
128 elements			
S-S	8.0000	8.0000	8.0000
C-C	6.9283	7.1239	6.9283
C-H	7.3861	7.4968	7.3484
C-F	5.4338	5.7011	5.4338

Table 3.3 Percentage of error in L_2 norm for buckling and vibration problems of the mode shape for the use of assumed analytical functions with reference to finite element solution

	Buckling (%)	Vibration (%)
16 elements		
S-S	0.0000	0.0000
C-C	0.0000	2.7461
C-H	0.6902	1.9838
C-F	0.0000	4.1839
32 elements		
S-S	0.0000	0.0000
C-C	0.0000	2.7461
C-H	0.4022	1.9702
C-F	0.0000	4.6723
64 elements		
S-S	0.0000	0.0000
C-C	0.0000	2.7461
C-H	0.5522	2.0167
C-F	0.0000	4.7712
128 elements		
S-S	0.0000	0.0000
C-C	0.0000	2.7461
C-H	0.5103	2.0168
C-F	0.0000	4.9154

Table 3.4 Variation of Ω_1 and Ω_2 for beams subjected to end concentrated periodic axial load

μ	α = 0.0		α = 0.5		α = 0.8	
	Ω_1	Ω_2	Ω_1	Ω_2	Ω_1	Ω_2
0	2.0000 (2.00)*	2.0000 (2.00)	1.4142 (1.40)	1.4142 (1.40)	0.8944 (0.91)	0.8944 (0.91)
0.1	1.8973 (1.89)	2.0976 (2.09)	1.3416 (1.35)	1.4832 (1.48)	0.8485 (0.85)	0.9380 (0.95)
0.2	1.7888 (1.79)	2.1908 (2.18)	1.2649 (1.27)	1.5491 (1.56)	0.8000 (0.79)	0.9797 (0.98)
0.3	1.6733 (1.68)	2.2803 (2.28)	1.1832 (1.19)	1.6124 (1.62)	0.7483 (0.74)	1.0198 (1.04)
0.4	1.5491 (1.57)	2.3664 (2.37)	1.0954 (1.12)	1.6733 (1.69)	0.6928 (0.69)	1.0583 (1.08)
0.5	1.4142 (1.44)	2.4494 (2.47)	1.0000 (1.02)	1.7320 (1.78)	0.6324 (0.65)	1.0954 (1.11)

*Values given in the parentheses are read from the graph [18].

Table 3.5 Percentage of error of Ω_1 and Ω_2 for the beams subjected to end concentrated periodic axial load to the FE method [18]

μ	α = 0		α = 0.5		α = 0.8	
	Ω_1	Ω_2	Ω_1	Ω_2	Ω_1	Ω_2
0	0.00	0.00	1.00	1.00	-1.74	-1.74
0.1	0.38	0.36	-0.62	0.21	-0.17	-1.2
0.2	-0.06	0.49	-0.40	-0.70	1.25	-0.03
0.3	-0.40	0.01	-0.57	-0.47	1.10	-1.98
0.4	-1.34	-0.13	-2.24	-0.99	0.40	-2.05
0.5	-1.82	-0.84	-2.00	-2.77	-2.78	-1.33

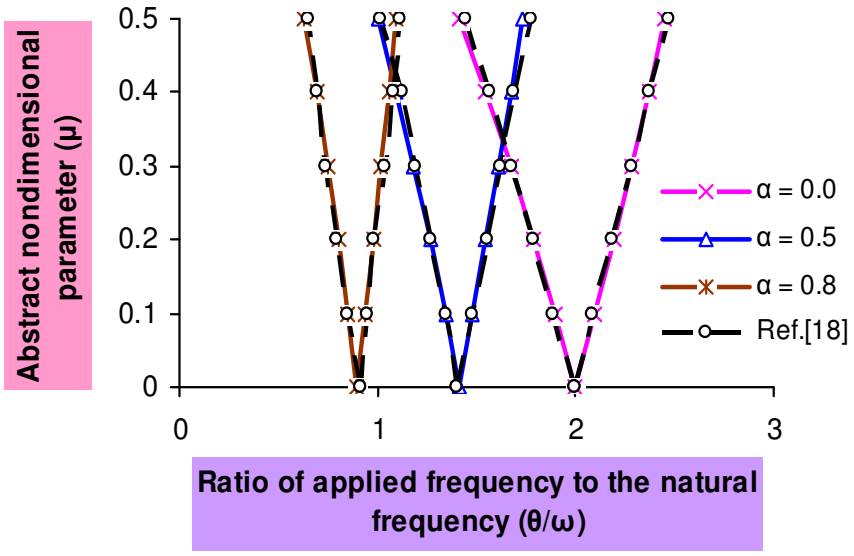

Fig. 3.6 Comparison of General dynamic stability curves for beams subjected to end concentrated periodic axial loads.

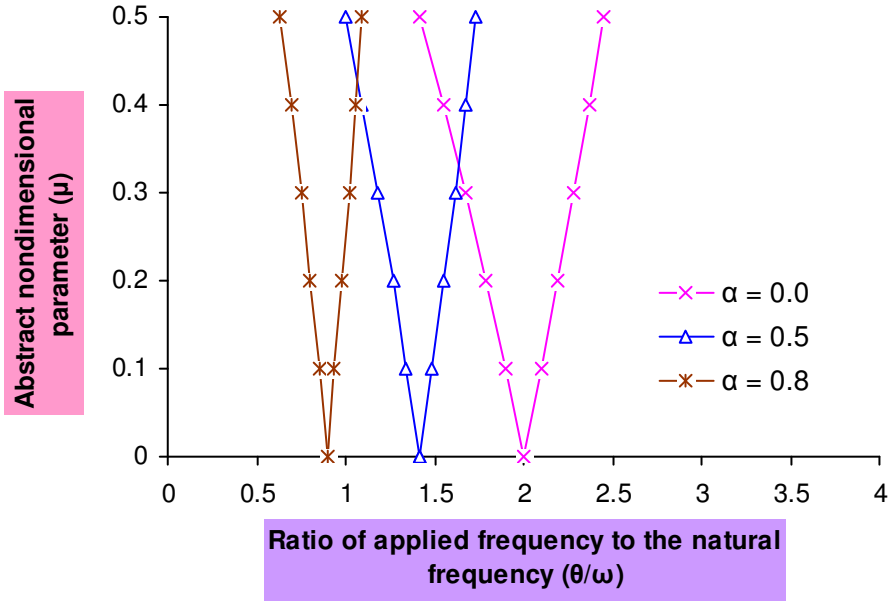

Fig.3.7 General dynamic stability curves for beams subjected to end concentrated periodic axial loads.

Table 3.6 Variation of $\Omega_1$and Ω_2 for one half sine wave for both stability and vibration for γ= 1 (γ< 4)*

μ	$\alpha = 0.0$		$\alpha = 0.5$		$\alpha = 0.8$	
	Ω_1	Ω_2	Ω_1	Ω_2	Ω_1	Ω_2
0.0	2.8284	2.8284	2.4494	2.4494	2.1908	2.1908
0.1	2.7568	2.8982	2.4083	2.4899	2.1725	2.2090
0.2	2.6832	2.9664	2.3664	2.5298	2.1540	2.2271
0.3	2.6076	3.0331	2.3237	2.5690	2.1354	2.2449
0.4	2.5298	3.0983	2.2803	2.6076	2.1166	2.2627
0.5	2.4494	3.1622	2.2360	2.6457	2.0976	2.2803

*λ_b and λ_f values for γ=0

Table 3.7 Variation of $\Omega_1$and Ω_2 for one half sine wave for both stability and vibration for γ= 2 (γ< 4)*

β	$\alpha = 0.0$		$\alpha = 0.5$		$\alpha = 0.8$	
	Ω_1	Ω_2	Ω_1	Ω_2	Ω_1	Ω_2
0.0	3.4641	3.4641	3.1622 (3.1439)[1]	3.1622 (3.1439)	2.9664	2.9664
0.2	3.4058	3.5213	3.0983 (3.0384)	3.2249 (3.1818)	2.8982	3.0331
0.4	3.3466	3.5777	3.0331 (3.0000)	3.2863 (3.2575)	2.8284	3.0983
0.6	3.2863	3.6331	2.9664 (2.9090)	3.3466 (3.3333)	2.7568	3.1622
0.8	3.2249	3.6878	2.8982 (2.8787)	3.4058 (3.4090)	2.6832	3.2249
1.0	3.1622	3.7416	2.8284 (2.8181)	3.4615 (3.4545)	2.6076	3.2863

[1]Values in the parenthesis are read from the graph [28]
*λ_b and λ_f values for γ=0

Table 3.8 Percentage of error of $\Omega_1$and Ω_2 for one half sine wave for both stability and vibration for γ= 2 (γ< 4)*

β	$\alpha = 0.5$	
	Ω_1	Ω_2
0.0	0.57	0.57
0.2	1.93	1.33
0.4	1.09	0.87
0.6	1.93	0.40
0.8	0.67	-0.09
1.0	0.36	0.20

*λ_b and λ_f values for γ=0

Table 3.9 Variation of $\Omega_1$and Ω_2 for one half sine wave for both stability and vibration for γ= 3 (γ< 4)*

μ	$\alpha = 0.0$		$\alpha = 0.5$		$\alpha = 0.8$	
	Ω_1	Ω_2	Ω_1	Ω_2	Ω_1	Ω_2
0.0	4.0000	4.0000	3.7416	3.7416	3.5777	3.5777
0.1	3.9496	4.0496	3.7148	3.7682	3.5665	3.5888
0.2	3.8987	4.0987	3.6878	3.7947	3.5552	3.6001
0.3	3.8471	4.1472	3.6606	3.8209	3.5441	3.6111
0.4	3.7947	4.1952	3.6331	3.8471	3.5327	3.6221
0.5	3.7416	4.2426	3.6055	3.8729	3.5213	3.6331

*λ_b and λ_f values for γ=0

Table 3.10 Variation of $\Omega_1$and Ω_2 for two half sine waves for the stability and one half sine wave for the vibration for γ= 4.5 (γ> 4)*

μ	$\alpha = 0.0$		$\alpha = 0.5$		$\alpha = 0.8$	
	Ω_1	Ω_2	Ω_1	Ω_2	Ω_1	Ω_2
0.0	4.6894	4.6894	3.6618	3.6618	2.8739	2.8739
0.1	4.5027	4.8690	3.5426	3.7771	2.8135	2.9330
0.2	4.3079	5.0422	3.4193	3.8891	2.7519	2.9910
0.3	4.1038	5.2096	3.2915	3.9979	2.6888	3.0478
0.4	3.8891	5.3718	3.1584	4.1038	2.6241	3.1036
0.5	3.6618	5.5293	3.0195	4.2071	2.5579	3.1584

*λ_b and λ_f values for γ=0

Table 3.11 Variation of $\Omega_1$and Ω_2 for one half sine wave for both stability and vibration for γ= 2 (γ<4) ^

μ	$\alpha = 0.0$		$\alpha = 0.5$		$\alpha = 0.8$	
	Ω_1	Ω_2	Ω_1	Ω_2	Ω_1	Ω_2
0.0	3.4641	3.4641	2.4494	2.4494	1.5491	1.5491
0.1	3.2863	3.6331	2.3237	2.5690	1.4696	1.6248
0.2	3.0983	3.7947	2.1908	2.6832	1.3856	1.6970
0.3	2.8982	3.9496	2.0493	2.7928	1.2961	1.7663
0.4	2.6832	4.0987	1.8973	2.8982	1.2000	1.8330
0.5	2.4494	4.2426	1.7320	3.0000	1.0954	1.8973

^ λ_b value with γ and λ_f value for γ=0

Table 3.12 Variation of $\Omega_1$and Ω_2 for two half sine waves for the stability and one half sine wave for the vibration for γ= 4.5(γ> 4)^

μ	$\alpha = 0.0$		$\alpha = 0.5$		$\alpha = 0.8$	
	Ω_1	Ω_2	Ω_1	Ω_2	Ω_1	Ω_2
0.0	4.6904	4.6904	3.3166	3.3166	2.0976	2.0976
0.1	4.4497	4.9193	3.1464	3.4785	1.9899	2.2000
0.2	4.1952	5.1380	2.9664	3.6331	1.8761	2.2978
0.3	3.9242	5.3478	2.7748	3.7815	1.7549	2.3916
0.4	3.6331	5.5497	2.5690	3.9242	1.6248	2.4819
0.5	3.3166	5.7445	2.3452	4.0620	1.4832	2.5690

^ λ_b value with γ and λ_f value for γ=0

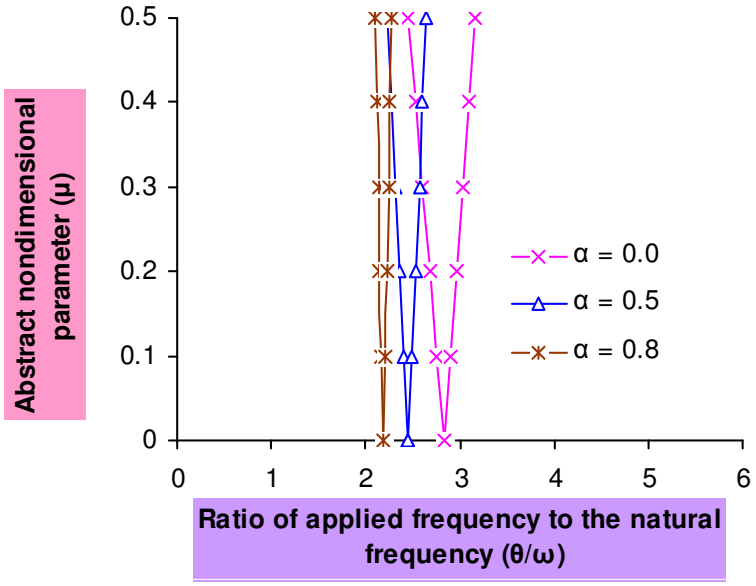

Fig.3.8 Dynamic stability curves for one half sine waves for both stability and vibration for γ=1(γ< 4)

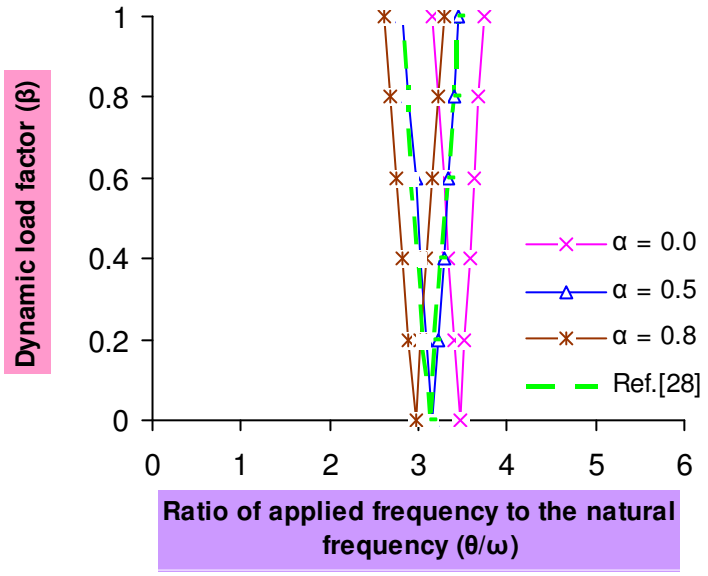

Fig.3.9 Dynamic stability curves for one half sine waves for both stability and vibration for γ= 2 (γ< 4)

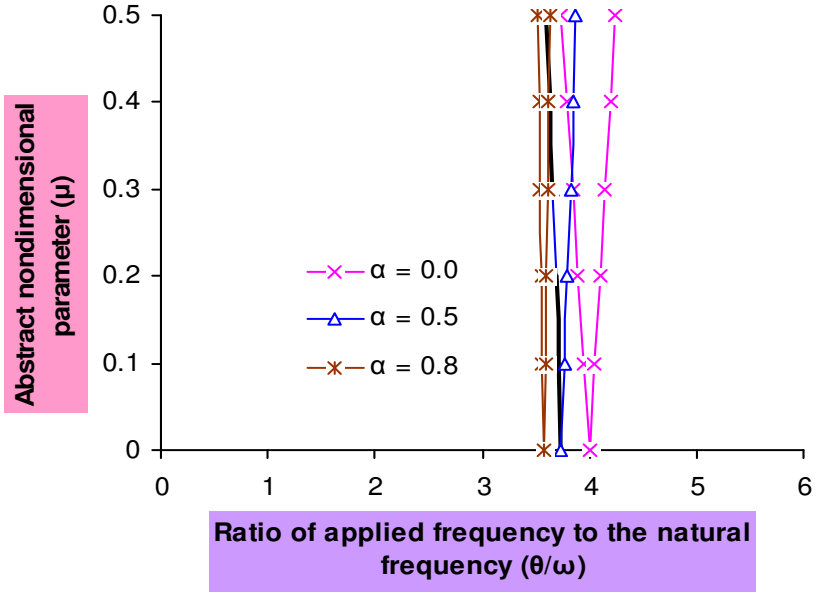

Fig.3.10 Dynamic stability curves for one half sine waves for both Stability and vibration for γ= 3 (γ< 4)

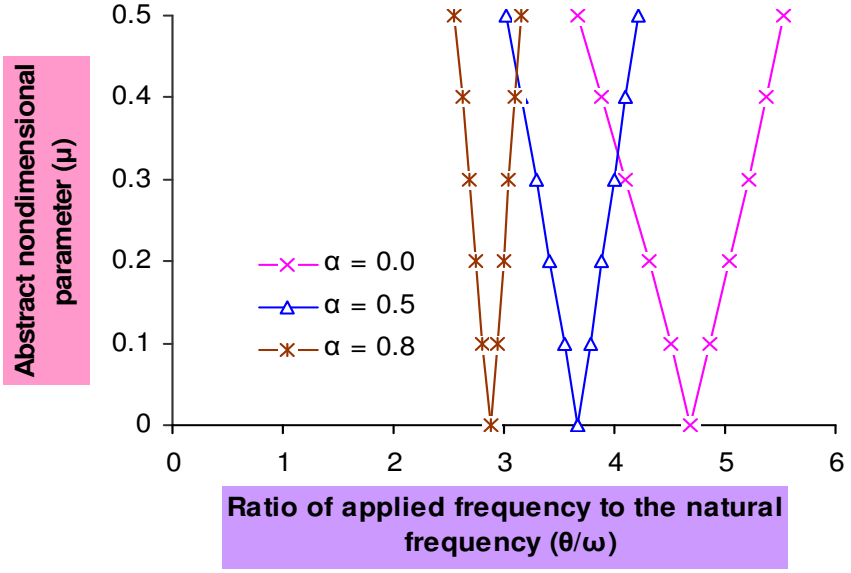

Fig.3.11 Dynamic stability curves for two half sine waves for stability and one half sine wave for vibration for γ= 4.5 (γ> 4)

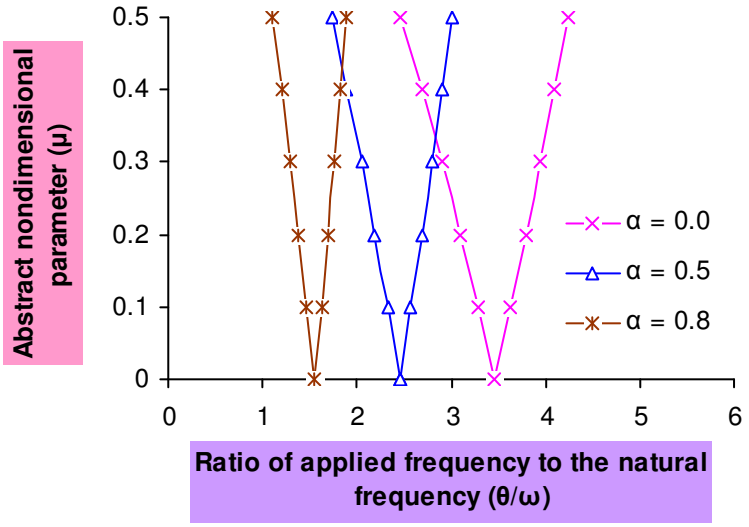

Fig.3.12 Dynamic stability curves for one half sine waves for both Stability and vibration for γ = 2(γ <4)

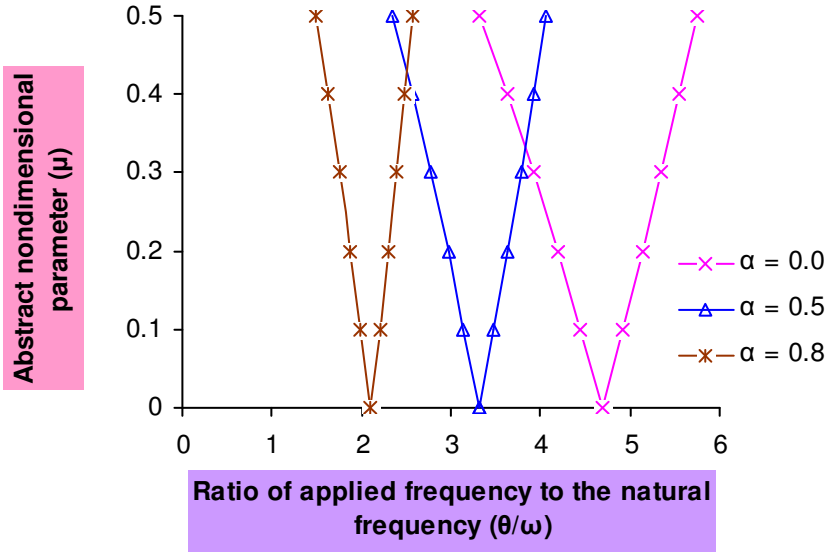

Fig.3.13 Dynamic stability curves for two half sine waves for stability and one half sine wave for vibration for γ = 4.5(γ > 4)

Table 3.13 Values of λ_b and λ_f for different values of γ_{F_1}, γ_{F_2}, m_b and m_f

γ_{F_1}	γ_{F_2}	m_b	λ_b	m_f	λ_f
0	0	1	9.8696	1	97.4090
2	0.1	1	30.5957	1	301.9681
2	0.2	1	31.5827	1	311.7090
3	0.1	1	40.4654	1	399.3770
3	0.2	1	41.4523	1	409.1181
4.5	0.1	2	51.5686	1	545.4909
4.5	0.2	2	52.5556	1	555.2310
5.5	0.1	2	54.0360	1	642.9000
5.5	0.2	2	55.0230	1	652.6409
5.5	0.1	2	54.0360	2	2133.2500
5.5	0.2	2	55.0230	2	2172.2227

Table 3.14 Variation of Ω_1 and Ω_2 for $m_b = m_f = 1$ with $\gamma_{F_1} = 2$ ($\gamma_{F_1} < \gamma_{T_1}$) and $\gamma_{F_2} = 0.1$

μ	$\alpha = 0.0$		$\alpha = 0.5$		$\alpha = 0.8$	
	Ω_1	Ω_2	Ω_1	Ω_2	Ω_1	Ω_2
0	3.5213	3.5213	3.2249	3.2249	3.0331	3.0331
0.1	3.4641	3.5777	3.1937	3.2557	3.0199	3.0463
0.2	3.4058	3.6331	3.1622	3.2863	3.0066	3.0594
0.3	3.3466	3.6878	3.1304	3.3166	2.9933	3.0724
0.4	3.2863	3.7416	3.0983	3.3466	2.9799	3.0854
0.5	3.2249	3.7947	3.0659	3.3763	2.9664	3.0983

Table 3.15 Variation of $\Omega_1$and Ω_2 for $m_b = m_f = 1$ with $\gamma_{F_1} = 2$ ($\gamma_{F_1} < \gamma_{T_1}$) and $\gamma_{F_2} = 0.2$

μ	$\alpha = 0.0$		$\alpha = 0.5$		$\alpha = 0.8$	
	Ω_1	Ω_2	Ω_1	Ω_2	Ω_1	Ω_2
0	3.5777	3.5777	3.2863	3.2863	3.0983	3.0983
0.1	3.5213	3.6331	3.2557	3.3166	3.0854	3.1112
0.2	3.4641	3.6878	3.2249	3.3466	3.0724	3.1240
0.3	3.4058	3.7416	3.1937	3.3763	3.0594	3.1368
0.4	3.3466	3.7947	3.1622	3.4058	3.0463	3.1496
0.5	3.2863	3.8470	3.1304	3.4351	3.0331	3.1622

Table 3.16 Variation of $\Omega_1$and Ω_2 for $m_b = m_f = 1$ with $\gamma_{F_1} = 3$ ($\gamma_{F_1} < \gamma_{T_1}$) and $\gamma_{F_2} = 0.1$

μ	$\alpha = 0.0$		$\alpha = 0.5$		$\alpha = 0.8$	
	Ω_1	Ω_2	Ω_1	Ω_2	Ω_1	Ω_2
0	4.0496	4.0496	3.7947	3.7947	3.6331	3.6331
0.1	4.0000	4.0987	3.7682	3.8209	3.6221	3.6441
0.2	3.9496	4.1472	3.7416	3.8470	3.6221	3.6441
0.3	3.8987	4.1952	3.7148	3.8729	3.6000	3.6660
0.4	3.8470	4.2426	3.6878	3.8987	3.5888	3.6769
0.5	3.7947	4.2895	3.6606	3.9242	3.5777	3.6878

Table 3.17 Variation of $\Omega_1$and Ω_2 for $m_b = m_f = 1$ with $\gamma_{F_1} = 3$ ($\gamma_{F_1} < \gamma_{T_1}$) and $\gamma_{F_2} = 0.2$

μ	$\alpha = 0.0$		$\alpha = 0.5$		$\alpha = 0.8$	
	Ω_1	Ω_2	Ω_1	Ω_2	Ω_1	Ω_2
0	4.0987	4.0987	3.847	3.847	3.6878	3.6878
0.1	4.0496	4.1472	3.8209	3.8729	3.6769	3.6986
0.2	4.0000	4.1952	3.7947	3.8987	3.6660	3.7094
0.3	3.9496	4.2426	3.7682	3.9242	3.6551	3.7202
0.4	3.8987	4.2895	3.7416	3.9496	3.6441	3.7309
0.5	3.8470	4.3358	3.7148	3.9749	3.6331	3.7416

Table 3.18 Variation of $\Omega_1$and Ω_2 for m_b = 2 and m_f = 1 with γ_{F_1} = 4.5 ($\gamma_{F_1} > \gamma_{T_1}$) and γ_{F_2} = 0.1

μ	$\alpha = 0.0$		$\alpha = 0.5$		$\alpha = 0.8$	
	Ω_1	Ω_2	Ω_1	Ω_2	Ω_1	Ω_2
0	4.7329	4.7329	3.7183	3.7183	2.9464	2.9464
0.1	4.5481	4.9107	3.6012	3.8319	2.8876	3.004
0.2	4.3555	5.0823	3.4801	3.9422	2.8276	3.0606
0.3	4.1545	5.2483	3.3546	4.0495	2.7663	3.1161
0.4	3.9422	5.4092	3.2243	4.154	2.7036	3.1707
0.5	3.7183	5.5658	3.0885	4.2559	2.6394	3.2243

Table 3.19 Variation of $\Omega_1$and Ω_2 for m_b = 2 and m_f = 1 with γ_{F_1} = 4.5 ($\gamma_{F_1} > \gamma_{T_1}$) and γ_{F_2} = 0.2

μ	$\alpha = 0.0$		$\alpha = 0.5$		$\alpha = 0.8$	
	Ω_1	Ω_2	Ω_1	Ω_2	Ω_1	Ω_2
0	4.7749	4.7749	3.7730	3.7730	3.0162	3.0162
0.1	4.5920	4.9510	3.6578	3.8849	2.9589	3.0725
0.2	4.4016	5.1210	3.5388	3.9936	2.9004	3.1277
0.3	4.2025	5.2856	3.4157	4.0994	2.8408	3.1820
0.4	3.9936	5.4452	3.2879	4.2025	2.7798	3.2354
0.5	3.7730	5.6002	3.1550	4.3032	2.7175	3.2879

Table 3.20 Variation of $\Omega_1$and Ω_2 for m_b = 2 and m_f = 1 with γ_{F_1} = 5.5 ($\gamma_{F_1} > \gamma_{T_1}$) and γ_{F_2} = 0.1

μ	$\alpha = 0.0$		$\alpha = 0.5$		$\alpha = 0.8$	
	Ω_1	Ω_2	Ω_1	Ω_2	Ω_1	Ω_2
0	5.1379	5.1379	4.0933	4.0933	3.3119	3.3119
0.1	4.9467	5.3223	3.9737	4.2094	3.2531	3.3696
0.2	4.7477	5.5005	3.8505	4.3224	3.1933	3.4264
0.3	4.5401	5.6732	3.7231	4.4326	3.1323	3.4822
0.4	4.3224	5.8407	3.5913	4. 5401	3.0701	3.5372
0.5	4.0933	6.0035	3.4544	4.6451	3.0066	3.5913

Table 3.21 Variation of $\Omega_1$and Ω_2 for m_b= 2 and m_f = 1 with γ_{F_1} = 5.5 ($\gamma_{F_1} > \gamma_{T_1}$) and γ_{F_2} = 0.2

μ	$\alpha = 0.0$		$\alpha = 0.5$		$\alpha = 0.8$	
	Ω_1	Ω_2	Ω_1	Ω_2	Ω_1	Ω_2
0	5.1767	5.1767	4.1454	4.1454	3.3787	3.3787
0.1	4.9875	5.3592	4.0277	4.2597	3.3213	3.4351
0.2	4.7909	5.5357	3.9066	4.3711	3.2629	3.4907
0.3	4.5858	5.7067	3.7815	4.4798	3.2034	3.5453
0.4	4.3711	5.8728	3.6611	4.5858	3.1428	3.5991
0.5	4.1454	6.0343	3.5181	4.6895	3.0810	3.6522

Table 3.22 Variation of $\Omega_1$and Ω_2 for m_b = m_f = 2 with γ_{F_1} = 5.5 ($\gamma_{F_1} > \gamma_{T_1}$) and γ_{F_2} = 0.1

μ	$\alpha = 0.0$		$\alpha = 0.5$		$\alpha = 0.8$	
	Ω_1	Ω_2	Ω_1	Ω_2	Ω_1	Ω_2
0	2.3398	2.3398	1.8640	1.8640	1.5082	1.5082
0.1	2.2527	2.4237	1.8096	1.9169	1.4814	1.5345
0.2	2.1621	2.5049	1.7535	1.9684	1.4542	1.5603
0.3	2.0675	2.5835	1.6955	2.0186	1.4264	1.5858
0.4	1.9684	2.6598	1.6354	2.0675	1.3981	1.6108
0.5	1.8640	2.7340	1.5731	2.1153	1.3692	1.6354

Table 3.23 Variation of $\Omega_1$and Ω_2 curves for m_b = m_f = 2 with γ_{F_1} = 5.5 ($\gamma_{F_1} > \gamma_{T_1}$) and γ_{F_2} = 0.2

μ	$\alpha = 0.0$		$\alpha = 0.5$		$\alpha = 0.8$	
	Ω_1	Ω_2	Ω_1	Ω_2	Ω_1	Ω_2
0	2.3611	2.3611	1.8907	1.8907	1.5410	1.5410
0.1	2.2748	2.4443	1.8370	1.9428	1.5148	1.5667
0.2	2.1851	2.5248	1.7817	1.9936	1.4882	1.5921
0.3	2.0916	2.6028	1.7247	2.0432	1.4610	1.6170
0.4	1.9936	2.6785	1.6657	2.0916	1.4334	1.6415
0.5	1.8907	2.7522	1.6046	2.1388	1.4052	1.6657

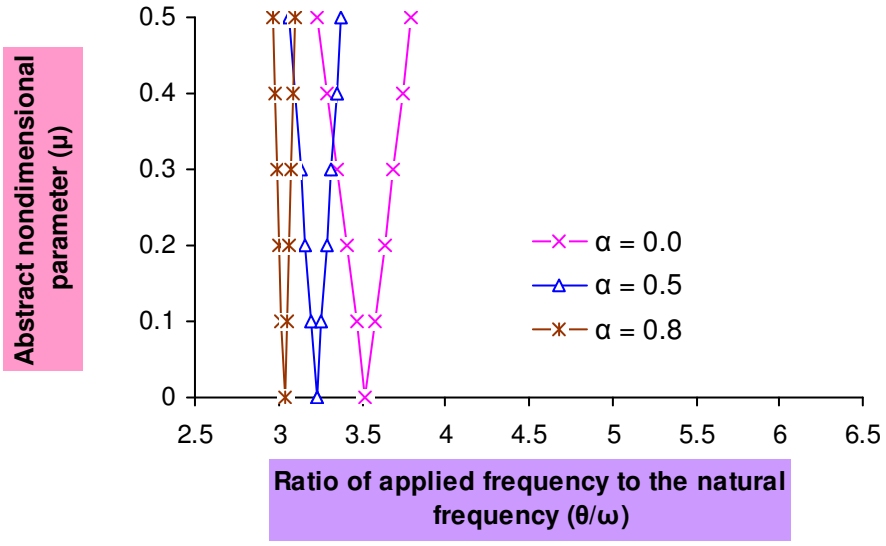

Fig. 3.14 Dynamic stability curves for m_b = m_f = 1 with γ_{F_1} = 2($\gamma_{F_1} < \gamma_{T_1}$) and γ_{F_2} = 0.1

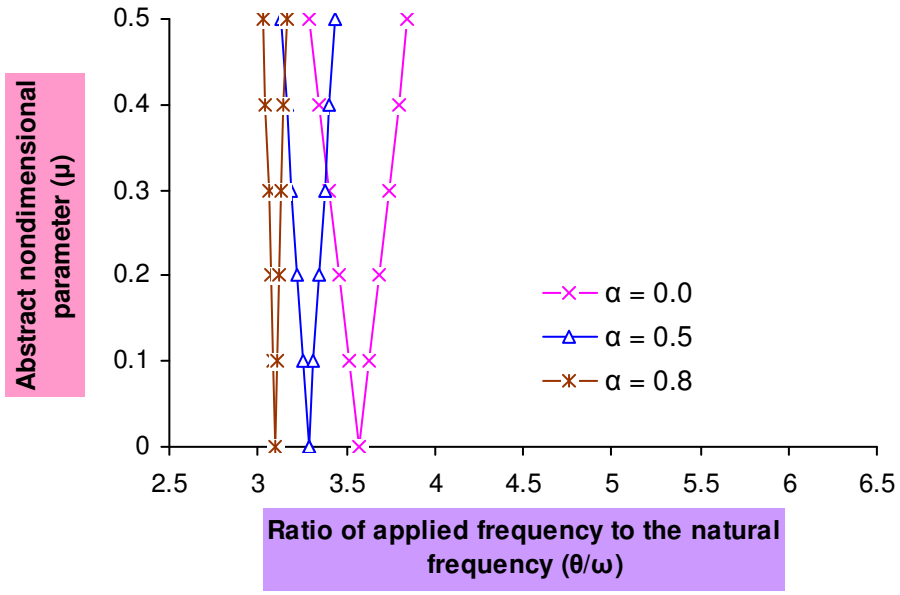

Fig. 3.15 Dynamic stability curves for m_b = m_f = 1 with γ_{F_1} = 2 ($\gamma_{F_1} < \gamma_{T_1}$) and γ_{F_2} = 0.2

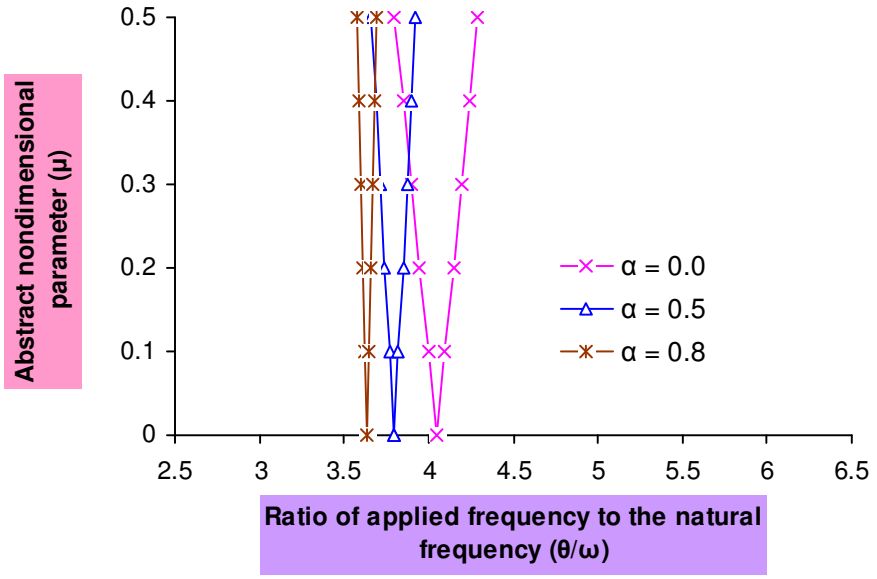

Fig. 3.16 Dynamic stability curves for m_b = m_f = 1 with γ_{F_1} = 3($\gamma_{F_1} < \gamma_{T_1}$) and γ_{F_2} = 0.1

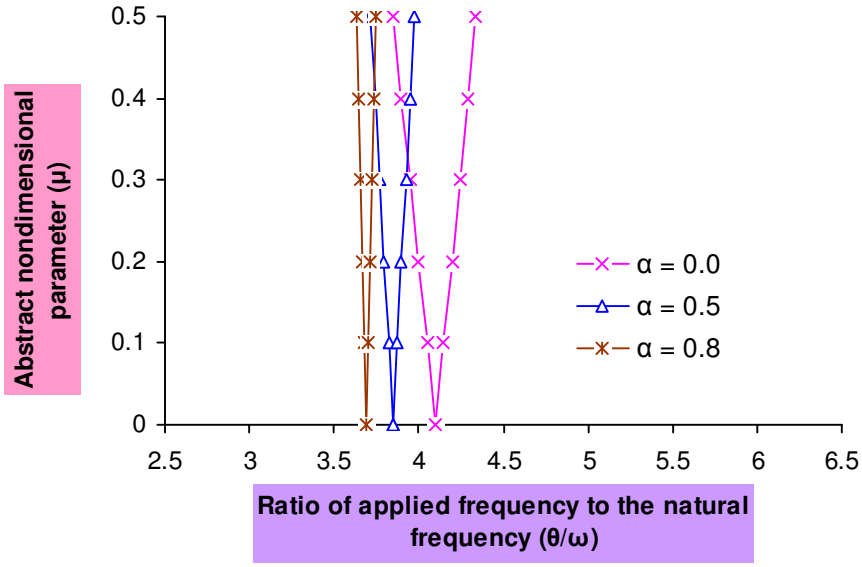

Fig.3. 17 Dynamic stability curves for m_b = m_f = 1 with γ_{F_1} = 3($\gamma_{F_1} < \gamma_{T_1}$) and γ_{F_2} = 0.2

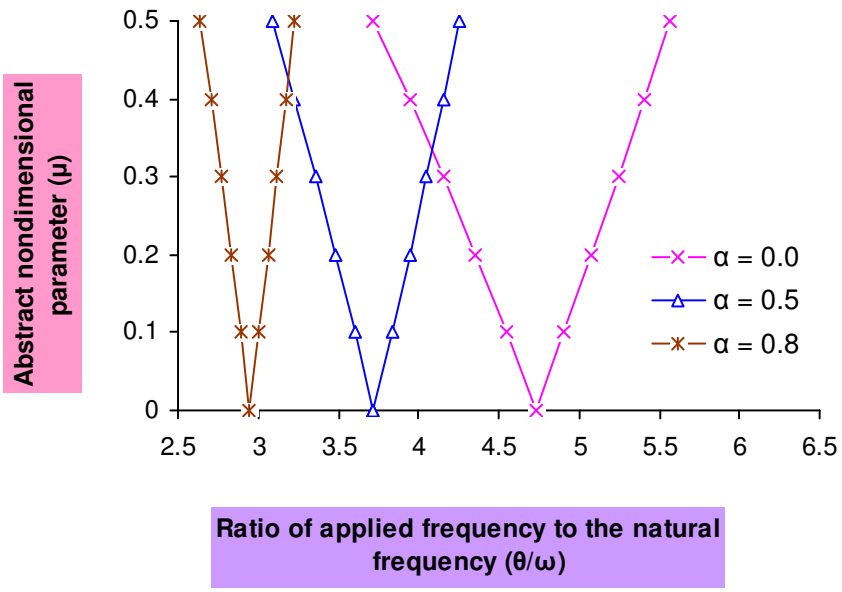

Fig.3.18 Dynamic stability curves for m_b = 2 and m_f = 1 with γ_{F_1} = 4.5 ($\gamma_{F_1} > \gamma_{T_1}$) and γ_{F_2} =0.1

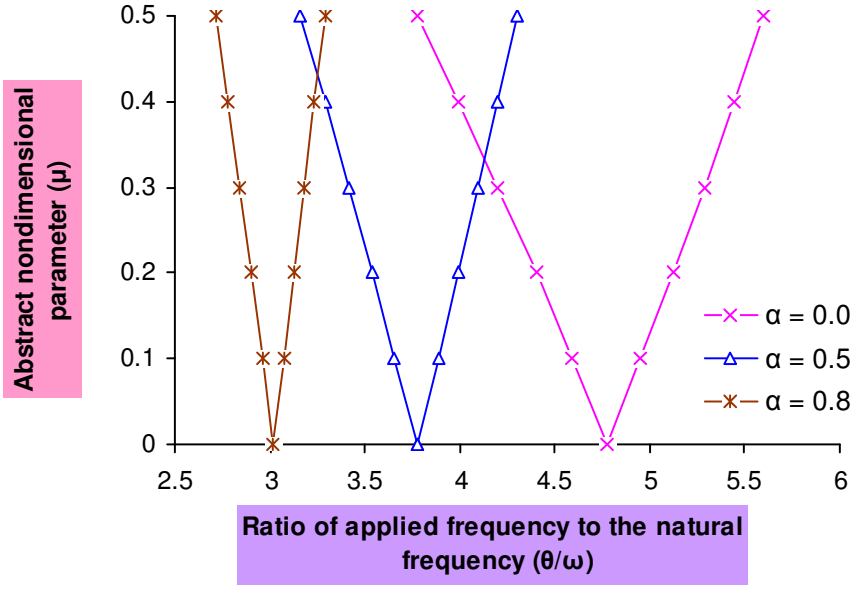

Fig.3.19 Dynamic stability curves for m_b = 2 and m_f = 1 with γ_{F_1} = 4.5 ($\gamma_{F_1} > \gamma_{T_1}$) and γ_{F_2} = 0.2

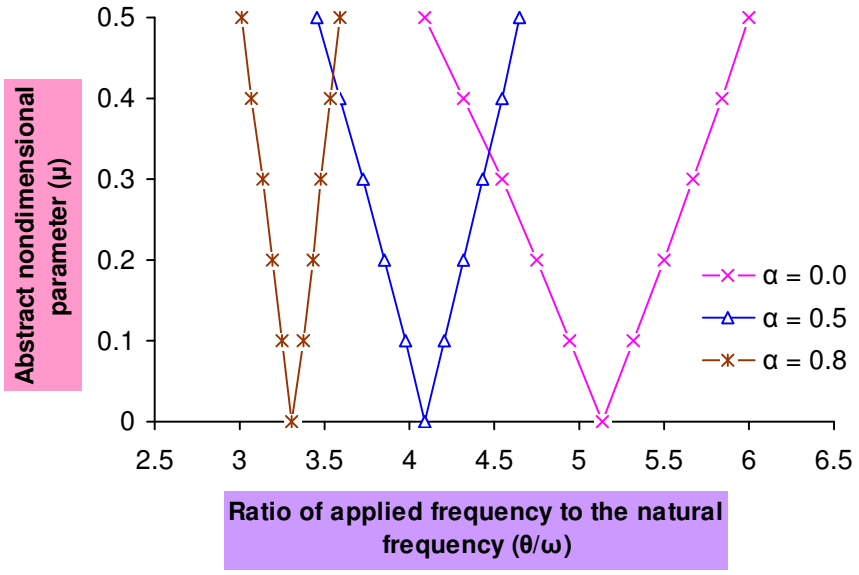

Fig. 3.20 Dynamic stability curves for m_b = 2 and m_f = 1 with γ_{F_1} = 5.5 ($\gamma_{F_1} > \gamma_{T_1}$) and γ_{F_2} = 0.1

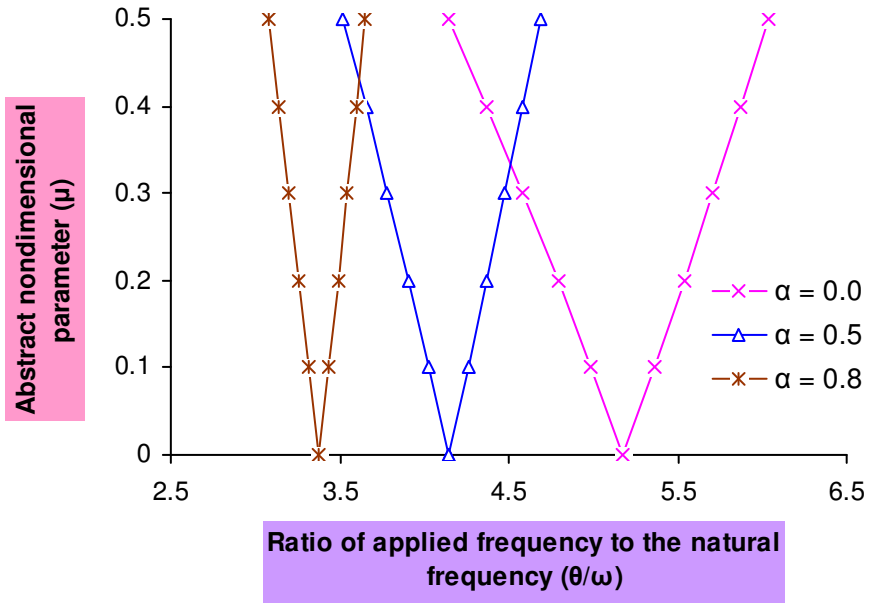

Fig.3.21 Dynamic stability curves for m_b=2 and m_f = 1 with γ_{F_1} = 5.5 ($\gamma_{F_1} > \gamma_{T_1}$) and γ_{F_2} = 0.2

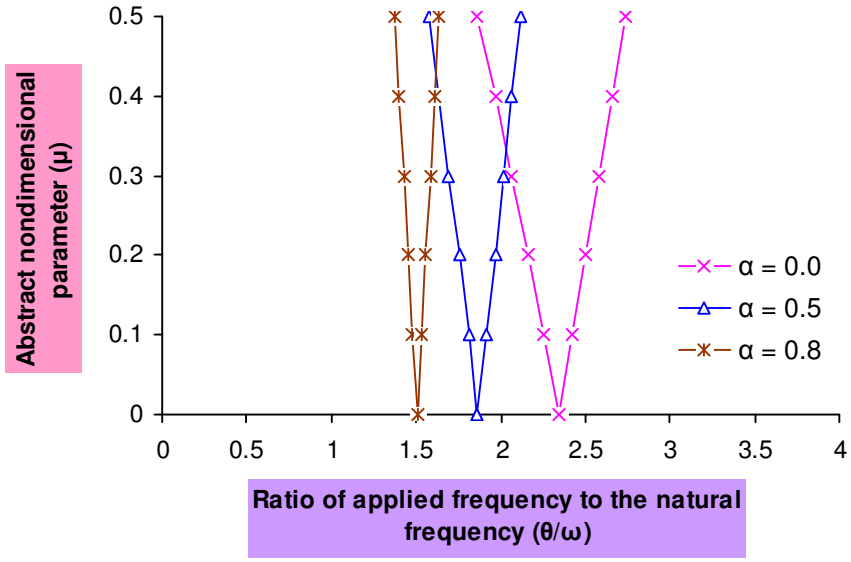

Fig.3.22 Dynamic stability curves for m_b = m_f = 2 with γ_{F_1} = 5.5 ($\gamma_{F_1} > \gamma_{T_1}$) and γ_{F_2} = 0.1

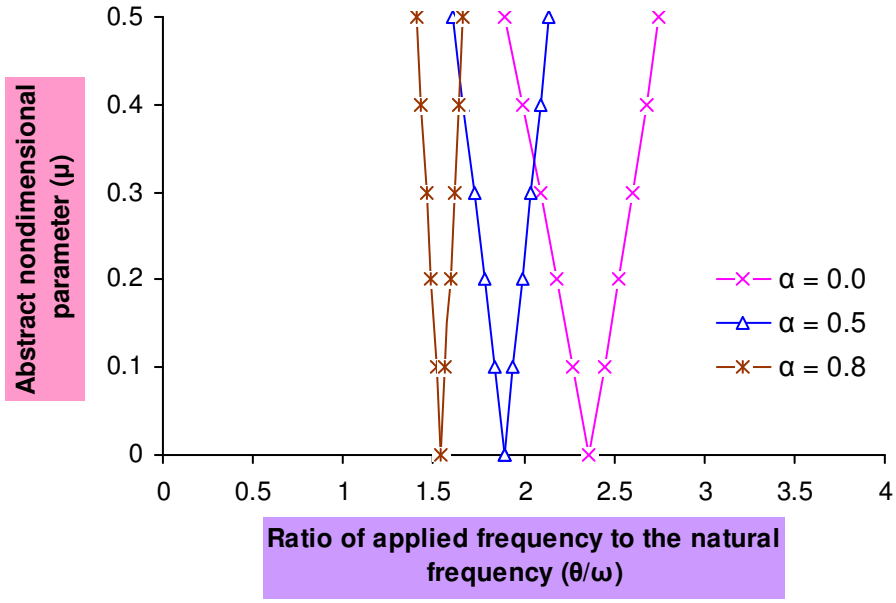

Fig. 3.23 Dynamic stability curves for m_b = m_f = 2 with γ_{F_1} = 5.5 ($\gamma_{F_1} > \gamma_{T_1}$) and γ_{F_2} = 0.2

Table 3.24 Variations of Ω_1 and Ω_2 for Beams Subjected to Periodic and Tensile Static Axial Loads

β	a = 0.0		a = 0.5		a =1.0		a =4.0	
	Ω_1	Ω_2	Ω_1	Ω_2	Ω_1	Ω_2	Ω_1	Ω_2
0.0	2.0000	2.0000	2.0000	2.0000	2.0000	2.0000	2.0000	2.0000
0.1	1.9493	2.0493	1.9667	2.0330	1.9748	2.0248	1.9989	2.0009
0.2	1.8973	2.0976	1.9328	2.0655	1.9493	2.0493	1.9979	2.0019
0.3	1.8439	2.1447	1.8984	2.0975	1.9235	2.0736	1.9969	2.0029
0.4	1.7888	2.1908	1.8633	2.1290	1.8973	2.0976	1.9959	2.0039
0.5	1.7320	2.2360	1.8275	2.1600	1.8708	2.1213	1.9949	2.0049
0.6	1.6733	2.2803	1.7910	2.1907	1.8439	2.1447	1.9939	2.0059
0.7	1.6124	2.3237	1.7538	2.2209	1.8165	2.1679	1.9929	2.0069
0.8	1.5491	2.3664	1.7158	2.2506	1.7888	2.1908	1.9919	2.0079
0.9	1.4832	2.4083	1.6769	2.2800	1.7606	2.2135	1.9909	2.0089
1.0	1.4142	2.4493	1.6334	2.3091	1.7320	2.2360	1.9899	2.0099

Table 3.25 Variation of Ω_1 and Ω_2 for Beams Subjected to Periodic and Tensile Static Axial Loads

μ	α = 0		α = 0.5		α = 0.8	
	Ω_1	Ω_2	Ω_1	Ω_2	Ω_1	Ω_2
0	2.0000 (2.00)*	2.0000 (2.00)	2.4494	2.4494	2.6832	2.6832
0.1	1.8973 (1.89)	2.0976 (2.09)	2.3237	2.5690	2.5455	2.8142
0.2	1.7888 (1.79)	2.1908 (2.18)	2.1908	2.6832	2.4000	2.9393
0.3	1.6733 (1.68)	2.2803 (2.28)	2.0493	2.7928	2.2449	3.0594
0.4	1.5491 (1.57)	2.3664 (2.37)	1.8973	2.8982	2.0784	3.1749
0.5	1.4142 (1.44)	2.4494 (2.47)	1.7320	3.0000	1.8973	3.2863

*Values given in the parentheses are read from the graph [18]

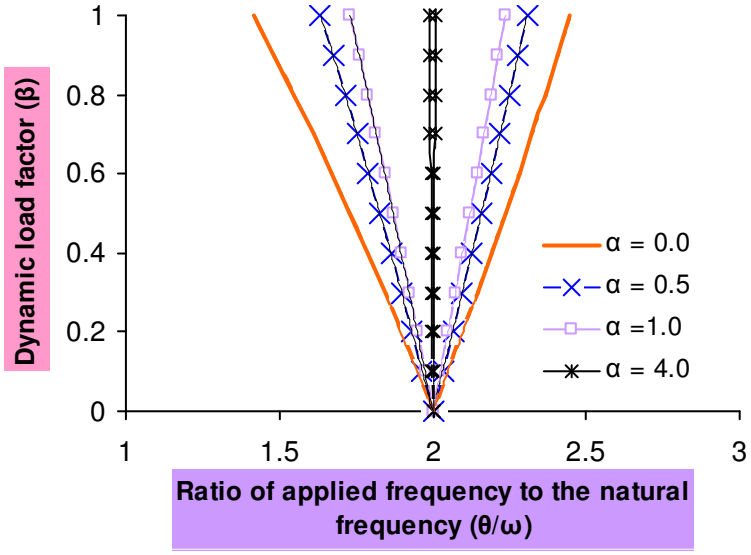

Fig.3.24 Alternate general dynamic stability curves with tensile static load

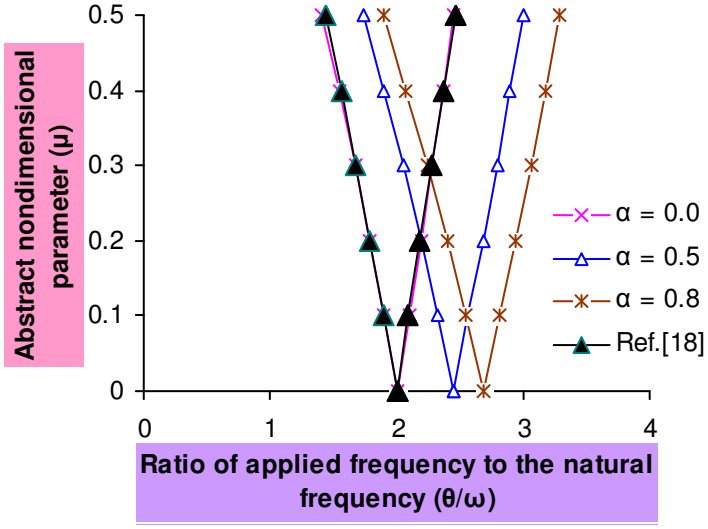

Fig.3.25 General dynamic stability curves with tensile static load

Table 3.26 Variation of Ω_1 and Ω_2 for square plate subjected to uniaxial compression without static compressive load (L_R = 0.0)

β	α = 0.0		α = 0.25		α = 0.5	
	Ω_1	Ω_2	Ω_1	Ω_2	Ω_1	Ω_2
0.0	2.0000	2.0000	1.7320	1.7320	1.4142	1.4142
0.1	1.9493	2.0493	1.6733	1.7888	1.3416	1.4832
0.2	1.8973	2.0976	1.6124	1.8439	1.2649	1.5491
0.3	1.8473	2.1447	1.5491	1.8973	1.1832	1.6124
0.4	1.7888	2.1908	1.4832	1.9493	1.0954	1.6733
0.5	1.7320	2.2360	1.4142	2.0000	1.0000	1.7320
0.6	1.6733	2.2803	1.3416	2.0493	0.8944	1.7888
0.7	1.6124	2.3237	1.2649	2.0976	0.7745	1.8439
0.8	1.5491	2.3664	1.1832	2.1447	0.6324	1.8973
0.9	1.4832	2.4083	1.0954	2.1908	0.4472	1.9493
1.0	1.4142	2.4493	1.0000	2.2360	0.0000	2.0000

Table 3.27 Variation of Ω_1 and Ω_2 for square plate subjected to uniaxial Periodic load for α = 0

β	Present study		Ramachandra & Sarat Kumar[93][1]	
	Ω_1	Ω_2	Ω_1	Ω_2
0.0	39.4801	39.4801	39.09	39.09
0.1	38.4790	40.4531	38.63	40.00
0.2	37.4527	41.4066	37.27	40.91
0.3	36.4657	42.3363	36.59	42.04
0.4	35.3109	43.2463	35.22	42.73
0.5	34.1890	44.1386	34.54	43.64
0.6	33.0309	45.0131	32.72	44.54
0.7	31.8287	45.8698	31.81	45.45
0.8	30.5792	46.7127	30.68	46.36
0.9	29.2783	47.5398	29.45	46.81
1.0	27.9163	48.3491	29.27	47.72

[1]Values are read from the graph [93]

Table 3.28 Variation of Ω_1 and Ω_2 for square plate subjected to uniaxial Periodic load for α = 0.6

β	Present Formula		Ramachandra & Sarat Kumar[93][1]	
	Ω_1	Ω_2	Ω_1	Ω_2
0.0	24.9693	24.9693	25.03	25.03
0.05	24.1755	25.7370	24.18	25.64
0.1	23.3563	26.4831	23.45	26.36
0.15	22.5055	27.2096	22.48	27.09
0.2	21.6231	27.9163	21.51	27.93
0.25	20.7033	28.6052	20.79	28.54
0.3	19.7393	29.2783	19.81	29.27

[1]Values are read from the graph [93]

Table 3.29 Variation of Ω_1 and Ω_2 for square plate subjected to the applied compressive load system with static compressive load ratio (L_R = 0.5)

β	α = 0.0		α = 0.25		α = 0.5	
	Ω_1	Ω_2	Ω_1	Ω_2	Ω_1	Ω_2
0.0	1.6329	1.6329	1.4142	1.4142	1.1547	1.1547
0.1	1.5916	1.6733	1.3662	1.4605	1.0954	1.2110
0.2	1.5491	1.7126	1.3165	1.5055	1.0327	1.2649
0.3	1.5055	1.7511	1.2649	1.5491	0.9660	1.3165
0.4	1.4605	1.7888	1.2110	1.5916	0.8944	1.3662
0.5	1.4142	1.8257	1.1547	1.6329	0.8164	1.4142
0.6	1.3662	1.8618	1.0954	1.6733	0.7302	1.4605
0.7	1.3165	1.8973	1.0327	1.7126	0.6324	1.5055
0.8	1.2649	1.9321	0.9660	1.7511	0.5163	1.5491
0.9	1.2110	1.9663	0.8944	1.7888	0.3651	1.5916
1.0	1.1547	2.0000	0.8164	1.8257	0.0000	1.6329

Table 3.30 Variation of Ω_1 and Ω_2 for square plate subjected to the applied compressive load system with static compressive load ratio (L_R = 1.0)

β	α = 0.0		α = 0.25		α = 0.5	
	Ω_1	Ω_2	Ω_1	Ω_2	Ω_1	Ω_2
0.0	1.4142	1.4142	1.2247	1.2247	1.0000	1.0000
0.1	1.3784	1.4491	1.1832	1.2649	0.9486	1.0488
0.2	1.3416	1.4832	1.1401	1.3038	0.8944	1.0954
0.3	1.3038	1.5165	1.0954	1.3416	0.8366	1.1401
0.4	1.2649	1.5491	1.0488	1.3784	0.7745	1.1832
0.5	1.2247	1.5811	1.0000	1.4142	0.7071	1.2247
0.6	1.1832	1.6124	0.9486	1.4491	0.6324	1.2649
0.7	1.1401	1.6431	0.8944	1.4832	0.5477	1.3038
0.8	1.0954	1.6733	0.8366	1.5165	0.4472	1.3416
0.9	1.0488	1.7029	0.7745	1.5491	0.3162	1.3784
1.0	1.0000	1.7320	0.7071	1.5811	0.0000	1.4142

Table 3.31 Variation of Ω_1 and Ω_2 for square plate subjected to uniaxial periodic load without static compressive load (L_R = 0.0)

μ	α = 0.0		α = 0.5		α = 0.8	
	Ω_1	Ω_2	Ω_1	Ω_2	Ω_1	Ω_2
0.0	2.0000	2.0000	1.4142	1.4142	0.8944	0.8944
0.1	1.8973	2.0976	1.3416	1.4832	0.8485	0.9380
0.2	1.7888	2.1908	1.2649	1.5491	0.8000	0.9797
0.3	1.6733	2.2803	1.1832	1.6124	0.7483	1.0198
0.4	1.5491	2.3664	1.0954	1.6733	0.6928	1.0583
0.5	1.4142	2.4494	1.0000	1.7320	0.6324	1.0954

Table 3.32 Variation of Ω_1 and Ω_2 for square plate subjected to the applied compressive load system with static compressive load ratio (L_R = 0.5)

μ	α = 0.0		α = 0.5		α = 0.8	
	Ω_1	Ω_2	Ω_1	Ω_2	Ω_1	Ω_2
0.0	1.6329	1.6329	1.1546	1.1546	0.7302	0.7302
0.1	1.5490	1.7126	1.0953	1.2109	0.6927	0.7658
0.2	1.4604	1.7889	1.0287	1.2647	0.6531	0.8000
0.3	1.3661	1.8617	0.9660	1.3164	0.6109	0.8326
0.4	1.2647	1.9322	0.8943	1.3661	0.5656	0.8640
0.5	1.1546	2.0000	0.8165	1.4140	0.5163	0.8943

Table 3.33 Variation of Ω_1 and Ω_2 for square plate subjected to the applied compressive load system with static compressive load ratio (L_R = 1.0)

μ	α = 0.0		α = 0.5		α = 0.8	
	Ω_1	Ω_2	Ω_1	Ω_2	Ω_1	Ω_2
0.0	1.4142	1.4142	1.0000	1.0000	0.6324	0.6324
0.1	1.3416	1.4832	0.9486	1.0488	0.6000	0.6633
0.2	1.2649	1.5491	0.8944	1.0954	0.5656	0.6928
0.3	1.1832	1.6124	0.8366	1.1401	0.5291	0.7211
0.4	1.0954	1.6733	0.7745	1.1832	0.4898	0.7483
0.5	1.0000	1.7320	0.7071	1.2247	0.4472	0.7745

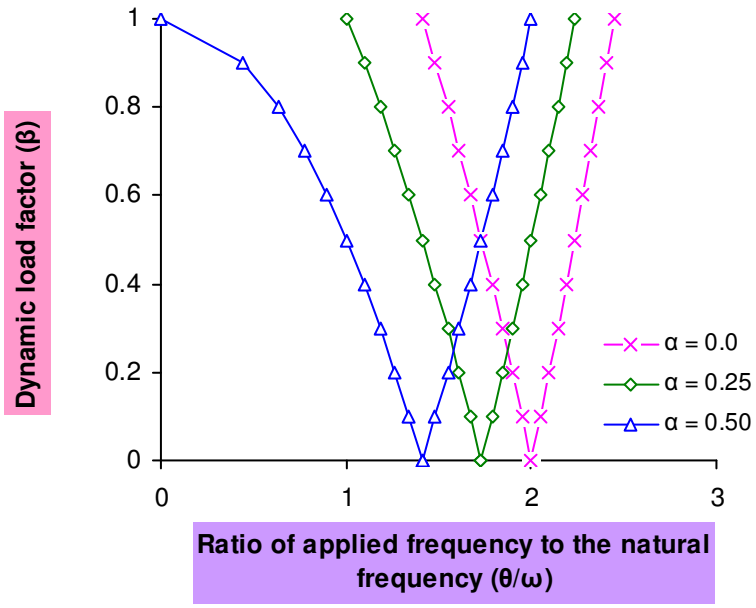

Fig.3.26 Alternate dynamic stability curves for square plate subjected to uniaxial compression without static compressive load (L_R = 0.0)

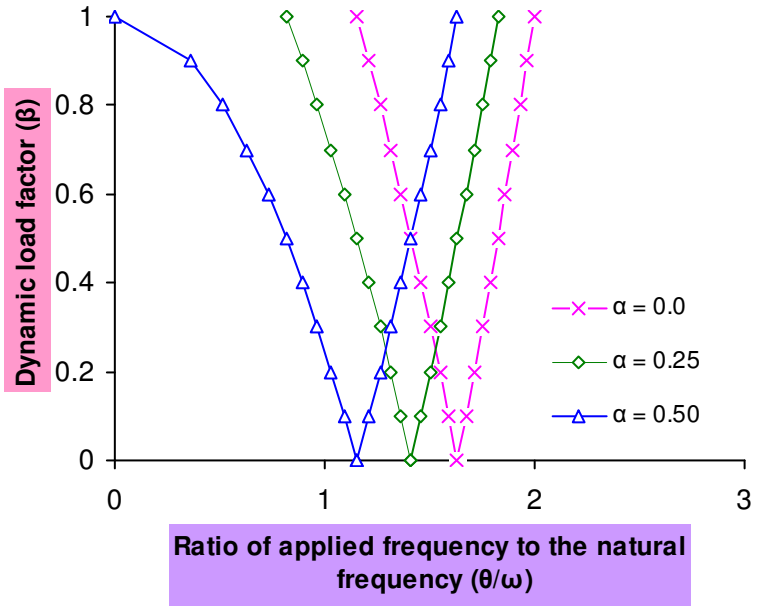

Fig.3.27 Alternate dynamic stability curves for square plate subjected to the applied compressive load system with static compressive load ratio (L_R = 0.5)

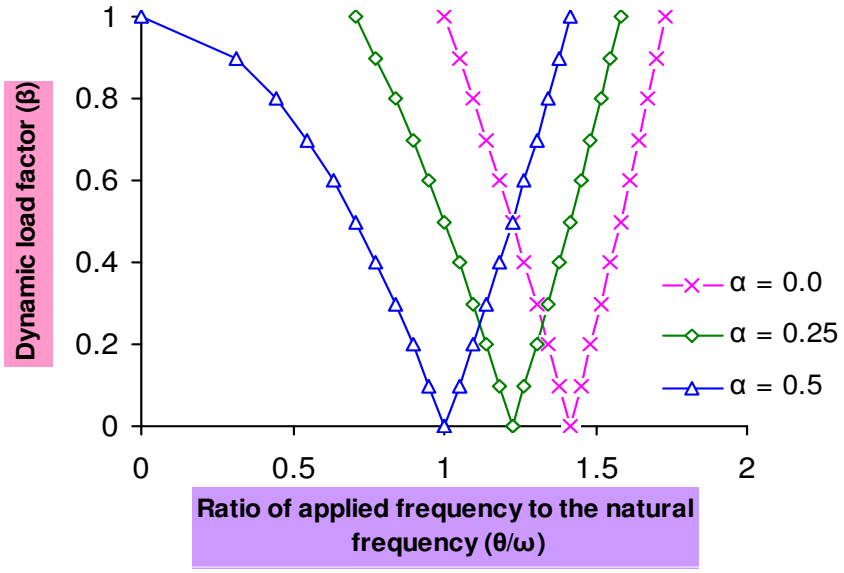

Fig.3.28 Alternate dynamic stability curves for square plate subjected to the applied compressive load system with static compressive load ratio (L_R = 1.0)

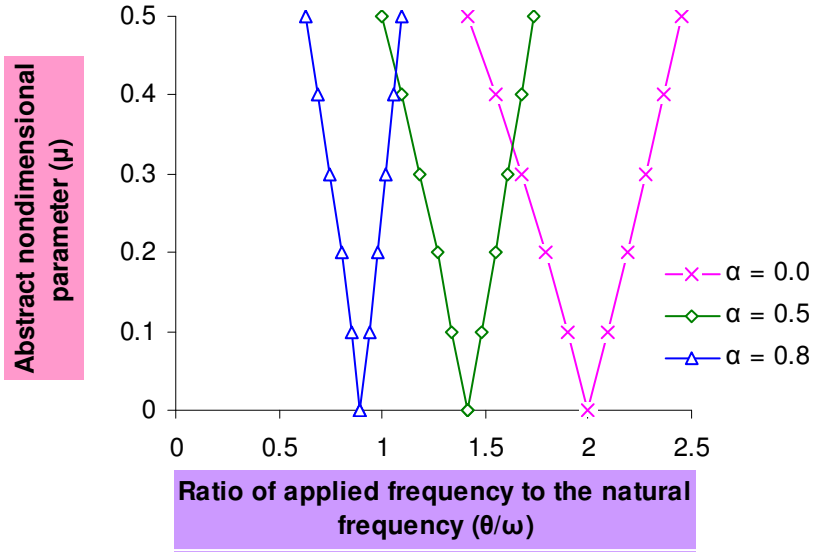

Fig.3.29 General Dynamic stability curves for square plate subjected to uniaxial compression without static compressive load (L_R = 0.0)

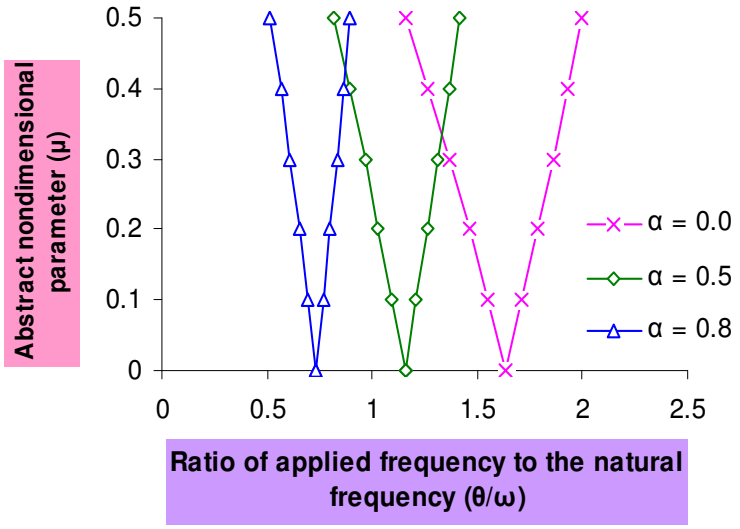

Fig. 3.30 General Dynamic stability curves for square plate subjected to the applied compressive load system with static compressive load ratio (L_R = 0.5)

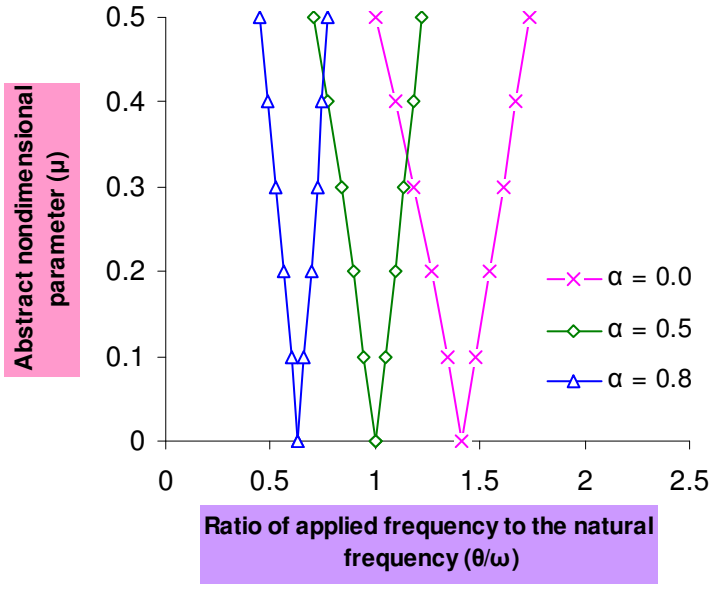

Fig.3.31 General Dynamic stability curves for square plate subjected to the applied compressive load system with static compressive load ratio (L_R = 1.0)